VEHICLE DESIGN PARAMETERS FOR AN ENTRY INTO THE ATMOSPHERE OF JUPITER

DICKINSON PRENTISS

VEHICLE DESIGN PARAMETERS FOR AN ENTRY INTO THE ATMOSPHERE OF JUPITER

by

Dickinson Prentiss, Lieutenant, United States Navy

B.S., Yale University, 1953

B.S., United States Naval Postgraduate School, 1959

Submitted in Partial Fulfillment

of the Requirements for the

Degree of Master of Science

at the

MASSACHUSETTS INSTITUTE OF TECHNOLOGY

June, 1960

VEHICLE DESIGN PARAMETERS FOR AN ENTRY INTO THE ATMOSPHERE OF JUPITER

by

Dickinson Prentiss, Lieutenant, U.S. Navy

Submitted to the Department of Aeronautics and Astronautics, Massachusetts Institute of Technology, on May 20, 1960, in partial fulfillment of the requirements for the degree of Master of Science.

ABSTRACT

A comprehensive analysis of the available literature on the atmosphere of Jupiter is made, and two models are selected as being most likely. It is suggested that a simple probe to Jupiter might resolve the question of which atmosphere actually exists.

The general ballistic entry equations are displayed, and specific solutions for direct and displaced orbital entries are made in two dimensions for Jupiter. It is found that a large dense vehicle, requiring the Saturn booster and utilizing a graphite ablative heat shield, can make a direct parabolic entry at angles up to 30°. It is doubtful that mid-course and terminal guidance exists which can give the precise injection angles required by this mission.

The feasibility of atmospheric determination by measurements of drag load factor, altitude, and heating rate is discussed. The general conclusion is that if a successful entry can be made, the atmosphere can be determined. The success of the entry depends on control of the entry angle.

Thesis Supervisor: Leon Trilling

Title: Associate Professor of
Aeronautics and Astronautics

ACKNOWLEDGMENTS

The author wishes to express his appreciation to the following persons: Associate Professors Leon Trilling and Holt Ashley for their advice and support, and Misses Maris Fisher and Betty Belknap for typing the manuscript.

The graduate work for which this thesis is a partial requirement was performed while the author was assigned by the United States Navy for graduate training at the Massachusetts Institute of Technology. The opinions and conclusions herein are those of the author, and publication of this thesis does not constitute approval by the Navy.

TABLE OF CONTENTS

TABLE OF CONTENTS (cont.)

OBJECT

The object of this thesis is to examine the vehicle design parameters for an entry into the atmosphere of Jupiter, and to investigate the feasibility of atmospheric determination by a simple entry vehicle.

CHAPTER 1

THE ATMOSPHERE OF JUPITER

1.1 Introduction

The purpose of this thesis is to examine the design parameters for a ballistic entry vehicle into the atmosphere of Jupiter. The first step is to determine the most probable model of the Jovian atmosphere.

The Jovian atmospheres are quite different from those of the Terrestrial planets. Jupiter is the closest and easiest to reach of these major planets, and therefore will provide Man's first experiment with such an atmosphere.

The most generally accepted theory of planetary formation is Kuiper's protoplanet theory (ref 1). The Solar nebula was broken up by gravitational instability and turbulence into the several protoplanets and the Sun. Condensation was already present, as the temperature of the gas in this nebula was much lower than that of the present planets. The heavy solid particles ranging from 10^{-5} to 10^{5} cm in diameter were drawn together to form the nucleus of the protoplanets. This only represented about one percent of the mass material. The heavier gases, notably oxygen, nitrogen, the noble gases, and the oxides of carbon, nitrogen and sulphur, were drawn toward the center and trapped. Many of the minerals

were carbonated, sulphated, and nitrated.

The remaining 99 percent of the mass in the gaseous envelope proceeded to evaporate due to the temperatures generated by contraction, and due to solar radiation on the nearer protoplanets. This envelope of Hydrogen, Helium, ammonia and methane completely evaporated from the Terrestrial planets. Some masses broke off due to the centrifugal force of high rotation, to later form the satellites of Earth and Mars. A few percent of the original envelope remained with the Jovian planets, however, and this accounts for their reducing hydrogen atmospheres. Jupiter retained approximately 10 percent of its protoplanet mass, and thus is the largest planet. Because of their higher velocities around the Sun, the outer planets lost more of their original envelope, thus they are smaller. It is believed that Pluto lost all of its gaseous envelope and therefore closely resembles Earth, except for its temperature.

Further contraction of the Terrestrial planets forced percolation and exhalation of gases from within the hot core, and this accounts for the Earth's oxidizing atmosphere. Such atmospheres as remain on the Terrestrial planets, then, are these secondary emissions of the heavy gases from within. Mercury lost most of its secondary atmosphere because of its size and proximity to the Sun. Venus apparently has lost most of its water due to solar proximity, and Mars has lost most of its atmosphere because of its small size.

The evaporation from the major planets continued for a shorter time than it did from the Terrestrial planets. Kuiper estimates 10^8 years for Earth, and 10^5 years for Jupiter. This is due to the lower temperature and greater distance from the Sun, and also to the larger

mass of Jupiter. The rate of evaporation depends on the log of the mass to radius ratio, and the temperature. Kuiper has shown that Jupiter lost considerable Hydrogen, and some Helium during the period of 10^5 years when it could lose it. At the present time, Jupiter is losing a negligible amount of gas. We should note that the loss in H_2 proceeds as the square of the loss of He, due to the masses of the two molecules. Therefore, contrary to the opinion of Urey (ref 2), considerably more Hydrogen could be lost than Helium.

We shall consider the atmosphere in more detail in the following sections. This should be our first experience with a reducing, light gas, "fuel" atmosphere.

1.2 The Ability to Hold an Atmosphere

According to the kinetic theory of gases (e.g., Jeans (ref 3)), an atmosphere in approximate isothermal equilibrium has the following density profile:

$$\rho = \rho_o e^{-\frac{mgr}{RT}\left(\frac{H}{r+H}\right)} \qquad (1\text{-}1)$$

where r = radius of planet, H = height above datum, and ρ_o = datum density.

Jeans also states that for stability over astronomical periods (10^9 years), the RMS molecular velocity of the gas at the exosphere should be less than 20 percent of the escape velocity, V_{esc}.

$$V_{esc} = \sqrt{\frac{2\,gM_J}{R_J + H}} \quad \frac{Ft.}{Sec.} \qquad (1\text{-}2)$$

For Jupiter, this works out to 64.6 km/sec. or 196,800 ft./sec!

At the present time, with temperatures of the order of 86°K, very few molecules at the escape level attain this velocity. However, during the protoplanet period, with temperatures of the order of 1000°K in the exosphere, and very low M/R ratios, efficient escape of H_2 would occur. According to Kuiper, the value of log M/R for Jupiter at the beginning of the evaporative period was -.39. The upper limit of log M/R permitting efficient escape is: +.18 for m = 2 (hydrogen), -.12 for m = 4 (helium), and -.77 for m = 18 (methane, ammonia). Thus we see that plenty of hydrogen, some helium, but no methane could have evaporated.

The other Jovian planets have less ability to hold their envelopes, and it is estimated that Saturn holds 2.5 percent and Uranus and Neptune about 1.25 percent. On this basis alone, Uranus and Neptune would be expected to have little or no hydrogen, which is not the case. However, it is believed that the extreme cold temperatures on these planets may have slowed diffusion of H_2 and He to the exosphere during the evaporation period. Their atmospheres also show a lack of turbulence which is present on Jupiter and Saturn. Their relative abundances cannot therefore be accurately predicted, but must be empirically determined. The usual assumption is that fractionation factors are some smooth function of m, the molecular weights of the constituents.

1.3 Probable Constituents

The composition of the protoplanets at the time of their formation is estimated to be in the solar or cosmic proportions. Accurate spectrographic analyses of the Sun and stars give the relative amounts of gaseous elements shown in Table I.

TABLE I

Initial Composition of Gaseous Envelope

Gas	Amount	Molecular Weight	Weight	% Weight
H_2	6289	2.016	12,679	63.5
He	1740	4.003	6,965	34.9
Ne	5.9	20.18	119	0.6
H_2O	3.75	18.02	68	0.34
NH_3	3.0	17.03	51	0.26
CH_4	1.4	16.04	22	0.11
A	0.8	36.3	29	0.15
Totals	8044		19,933	100 %

Average molecular weight, m = 2.48 $\qquad \gamma = 1.46$

Urey and others believe that the present remaining envelope of Jupiter contains hydrogen, helium and methane in these same proportions above the tropopause. To Kuiper it seems unlikely that the gases would remain so homogeneous, and would escape uniformly, leaving solar proportions intact. Kuiper holds that the gases would be fractioned in proportion to m_i , the molecular weight of each gas. These separate opinions lead to two different models of the atmosphere. To this writer, it seems more likely that Kuiper is correct, and this theory is supported by experimental evidence to be discussed later. However, we will carry both atmospheres through this thesis to provide a basis for

comparison of design parameters.

Urey's atmosphere, model "a", is shown below in Table II.

TABLE II

Solar Proportion Atmosphere, model a

Gas	Amount	Molecular Weight	Weight	% Weight
H_2	6289	2.016	12,679	64.4
He	1740	4.003	6,965	35.4
CH_4	1.4	16.04	22	0.2
Totals	8030		19,666	100 %
Average molecular weight, m = 2.47			γ = 1.47	

Kuiper's atmosphere, model b, is characterized by a reduction of Urey's model "a" by a factor such that the ratios of Hydrogen to Helium to Methane are:

$$6289n^2 : 1740n : 1.4$$
$$H_2 : He : CH_4 \qquad (1\text{-}3)$$

The factor n here is the reduction due to evaporation, and as pointed out before, H_2 evaporates as the square of He. To make the present mass come out right, and with the assumption of about 10 % of the protoplanet envelope remaining, $n \doteq .177$. Therefore, the model b atmosphere is reproduced in Table III.

We notice that to change the molecular weight by even this small amount requires a considerable change in the composition.

TABLE III

Reduced Proportion Atmosphere, model b

Gas	Amount	Molecular Weight	Weight	% Weight
H_2	197	2.016	396	23.9
He	308	4.003	1234	74.7
CH_4	1.4	16.04	22.5	1.4
Totals	506.4		1652.5	100.0%

Average molecular weight, m = 3.26 γ = 1.56

The pressures in the two models will vary considerably, as shown in the section on structure. These models are only for the gas above the tropopause, as it is assumed the heavier elements will have very low pressures at this height. Notice also that model b has He in excess of H_2 by 3 to 1, whereas in the solar proportions H_2 is over He by 2 to 1 by mass. Urey holds that such a great reduction in H_2 would be unlikely. Perhaps, then, the actual atmosphere is somewhere between these models, for surely some of the gas must have evaporated. We will carry both atmospheres through our calculations for comparison.

1.4 Methods of Measurement

The primary method used to determine atmospheric composition has been comparison of absorption spectrographs of the planet with emission spectrographs of the Sun. Absorption of a particular frequency line in the Sun's spectrum indicates the presence

of a particular gas. The strength of the absorption indicates the amount. This method has several drawbacks, however. It is limited in scope because the planets are not primary emitters; only the light from the Sun can be re-radiated. Certain gases like nitrogen and helium have no absorbtion lines in the useful range of spectrography. The Earth's atmosphere shuts out most of the ultra violet wavelengths. We also get interference from CO_2, H_2O, and oxygen in the Earth's atmosphere. Most of these hindrances can be avoided with careful work, but the most difficult of all is to obtain the laboratory comparison spectra of the various gases for identification.

Methane and ammonia bands were detected as early as 1932 by Wildt in the atmosphere of Jupiter. The ammonia band was much weaker than expected. It was then realized that the clouds on Jupiter were NH_3 cirrus, and less than one cm NPT* of free NH_3 existed above the cloudtops. According to Kuiper's protoplanet theory, the atmosphere should contain an abundance of H_2 and He, but no bands for these gases were identified. In 1938 Herzberg identified several lines around 7500 A° in the atmospheres of all the Jovian planets; and lines around 8270 A° in Uranus and Neptune. But it was not until 1952 that a laboratory experiment showed the 8270 A° lines to be pressure-induced quadruple vibration-rotation modes of the H_2 molecule. To reproduce this on Earth required a path length of 80 meters, a temperature of 78°K gained by cooling with liquid nitrogen, and a pressure of 100 atmospheres.

This illustrates the extremes in pressure, path length, and

---

* cm NPT = height in cm of equivalent column of the gas on Earth at normal pressure and temperature.

temperature that must be used to demonstrate on Earth the same lines found in nature's laboratory. It can be shown that the temperature on Jupiter at high pressures is too high to allow this excitation. But H_2 can be confirmed by its presence on Uranus and Neptune. The lines at 7500 A° are present on Jupiter, but have not to date been identified.

A rare but extremely important method of constitutive determination was the occultation of a star by Jupiter in November 1952. The rate of diminution of light from the star as it passes behind the planet is a function of the apparent motion, temperature, surface gravity, and mean molecular weight of the gases in the atmosphere. Since the first three of these parameters are fairly well known, the mean molecular weight can be found by photometric measurement of the rate of light diminution.

It was by this method that Baum and Code (ref 4) measured the m of Jupiter in 1952. The light curve best fit an atmosphere with m = 3.3. This was important confirmation that the primary constituents were H_2 and He, and CH_4 and NH_3 as indicated spectographically. It further indicates an abundance by weight of He over H_2 by 3:1 as predicted by Kuiper! This is why this author prefers Kuiper's model b atmosphere to Urey's model a.

Other methods of atmospheric measurement include ultraviolet and infrared absorption by the atmosphere, polarization, and radio emission. Although radio emission in a band around 22 mc has been detected from Jupiter, no conclusive evidence of composition has been found. Astronomers believe that this radiation is "static", caused by vast turbulence below the

clouds on Jupiter. According to Peek (ref 5) this turbulence gains its energy from heat within the planet, and from the fast planetary rotation. The turbulence accounts for the meteorological formation of the bands on the planet similar to the prevailing winds on Earth. This will be discussed more fully under Structures.

1.5 Structure of the Atmosphere

The general structure of both models will conform to the following assumptions:

1) A spherically symmetric atmosphere

2) Isothermal equilibrium in the stratosphere

3) Dry adiabatic lapse rate in troposphere

4) Moist (NH_3) adiabatic lapse rate below the cloud tops.

From these assumptions, the thermal models can be constructed as shown in figure 1. The isothermal temperature given by Peek (ref 5) is 86°K. The equilibrium temperature for solid NH_3 from the phase diagram is 165°K to 168°K, depending on pressure. Zero conditions refer to the tops of the clouds. The measurements of Jupiter's radius have always been referred to the cloud tops, so we will use this as zero altitude.

The dry adiabatic lapse rate is given by the expression:

$$\Gamma = \frac{m g_J}{R_g} \left(\frac{\gamma - 1}{\gamma}\right) \qquad (1\text{-}4)$$

This yields for Jupiter:

$$\Gamma_m = 2.47) = 2.6 \ ^\circ K/km$$

$$\Gamma_m = 3.26) = 4.0 \ ^\circ K/km$$

With this information, the depth of the cloud tops below the

tropopause is easily calculated. On the way down a level is passed which is at the radiometric temperature of Jupiter (102°K). This is the level which the thermocouple sees at 8-14μ. It is also the level where the pressure is approximately one atmosphere. The emissivity of the gases above this point is so low that we assume most of the energy radiated into space comes from below this level. Between here and the cloud tops there is less than one centimeter NPT of NH_3, and radiation from below the clouds is effectively blocked. This explains the rather weak ammonia absorption spectrographs from Jupiter.

The density ratio for the adiabatic portion of the atmosphere follows:

$$\sigma = \frac{\rho}{\rho_o} = \left(\frac{T}{T_o}\right)^{\left(\frac{1}{\gamma-1}\right)} = \frac{(T_o - r)H}{T_o}^{\left(\frac{1}{\gamma-1}\right)} \qquad (1\text{-}5)$$

The density, ρ_o, is calculated from the perfect gas law, which should apply at these temperatures and pressures.

$$\rho_o = \frac{\rho_o m}{R_g T_o} \qquad (1\text{-}6)$$

The pressures at the cloud tops are fixed by the $(H_2 + He/CH_4)$ abundance ratio used for model a and b.

ρ_o (m = 2.47) = 24 earth atmospheres

ρ_o (m = 3.26) = 2 earth atmospheres

Here we point out again that model b is more probable. The 8270 A° absorption due to H_2 quadruple excitation is absent from Jupiter. But if a pressure of 24 atm prevailed in the

clouds on Jupiter. According to Peek (ref 5) this turbulence gains its energy from heat within the planet, and from the fast planetary rotation. The turbulence accounts for the meteorological formation of the bands on the planet similar to the prevailing winds on Earth. This will be discussed more fully under Structures.

1.5 Structure of the Atmosphere

The general structure of both models will conform to the following assumptions:

1) A spherically symmetric atmosphere

2) Isothermal equilibrium in the stratosphere

3) Dry adiabatic lapse rate in troposphere

4) Moist (NH_3) adiabatic lapse rate below the cloud tops.

From these assumptions, the thermal models can be constructed as shown in figure 1. The isothermal temperature given by Peek (ref 5) is 86°K. The equilibrium temperature for solid NH_3 from the phase diagram is 165°K to 168°K, depending on pressure. Zero conditions refer to the tops of the clouds. The measurements of Jupiter's radius have always been referred to the cloud tops, so we will use this as zero altitude.

The dry adiabatic lapse rate is given by the expression:

$$\Gamma = \frac{mg_J}{R_g}\left(\frac{\gamma-1}{\gamma}\right) \qquad (1\text{-}4)$$

This yields for Jupiter:

$$\Gamma_m = 2.47 = 2.6 \text{ °K/km}$$

$$\Gamma_m = 3.26 = 4.0 \text{ °K/km}$$

With this information, the depth of the cloud tops below the

tropopause is easily calculated. On the way down a level is passed which is at the radiometric temperature of Jupiter (102°K). This is the level which the thermocouple sees at 8-14μ. It is also the level where the pressure is approximately one atmosphere. The emissivity of the gases above this point is so low that we assume most of the energy radiated into space comes from below this level. Between here and the cloud tops there is less than one centimeter NPT of NH_3, and radiation from below the clouds is effectively blocked. This explains the rather weak ammonia absorption spectrographs from Jupiter.

The density ratio for the adiabatic portion of the atmosphere follows:

$$\sigma = \frac{\rho}{\rho_o} = \left(\frac{T}{T_o}\right)^{\left(\frac{1}{\gamma-1}\right)} = \frac{(T_o - r)H}{T_o}^{\left(\frac{1}{\gamma-1}\right)} \qquad (1\text{-}5)$$

The density, ρ_o, is calculated from the perfect gas law, which should apply at these temperatures and pressures.

$$\rho_o = \frac{\rho_o m}{R_g T_o} \qquad (1\text{-}6)$$

The pressures at the cloud tops are fixed by the $(H_2 + He/CH_4)$ abundance ratio used for model a and b.

ρ_o (m = 2.47) = 24 earth atmospheres

ρ_o (m = 3.26) = 2 earth atmospheres

Here we point out again that model b is more probable. The 8270 A° absorption due to H_2 quadruple excitation is absent from Jupiter. But if a pressure of 24 atm prevailed in the

visible portion of the atmosphere, we probably could see this band.

Above the tropopause isothermal conditions are assumed to prevail. Therefore the density follows the expression:

$$\rho = \rho_{tr} e^{-K(H-H_{tr})} \qquad (1\text{-}7)$$

Here the scale height, $\frac{1}{K}$, is given by

$$K = \frac{g_J m}{R_g T g_E} \qquad (1\text{-}8)$$

Most references give the scale height of Jupiter as about 60,000 feet, but such a figure is based on a mean temperature of the planet of 170°K. Since the scale height is to be used over the isothermal portion of the atmosphere, this author prefers to use the isothermal temperature (86°K). This drops the figure down considerably, and in fact makes $\frac{1}{K}$ for model b = 26,000 feet. This compares with the value for Earth of 23,500 feet.

The density profiles are plotted in Figure 2 based on the above assumptions. We should note that the density for model b is almost identical with Earth. Therefore, the dynamic pressures are equal, and any winged vehicle which can fly above the Earth can also fly above Jupiter. Of course the pressures and lift required at a given altitude will be different.

1.6 Summary

Fairly conclusive evidence has been offered to support model b over model a. Comparing the surface of Earth to the tops of the clouds for Jupiter, one finds the density profiles nearly identical. Assuming an entry density at 160 kilometers for Earth, the same altitude would prevail for Jupiter. Even with model a, entry would

commence at about 250 kilometers. It is unlikely that any reasonable shape would penetrate below the clouds before the high Mach phase is over. Pressures increase very rapidly below the clouds, and the critical pressure for H_2 is reached at about -120 km. From this point on we have solid H_2 to a pressure of 200,000 atm., and metalic H_2 beyond. It seems unlikely that Earth people would ever explore Jupiter to a significant depth below the clouds. But it is quite likely that they will explore the upper atmosphere for scientific reasons. Jupiter is the closest and easiest to reach of the remaining protoplanets. The Terrestrial planets all have secondary atmospheres, but an accurate determination of Jupiter's atmosphere would give good evidence about the formation of the solar system.

Such an entry could be made with a rather unsophisticated probe at an early date. The potential required would be very little more than the recently launched Venus probe. Higher g forces and heating would be encountered due only to the higher entry velocities involved. Such an entry will be designed in the subsequent chapters.

TABLE IV

Summary of Atmospheric Characteristics

Property	Jupiter a	Jupiter b	Earth
T_o	165°K	168°K	288°K
ρ_o (slugs/ft.^{3})	8.2×10^{-3}	9.02×10^{-4}	2.7×10^{-3}
ρ_o (atm)	24	2	1
K (ft^{-1})	2.92×10^{-5}	3.84×10^{-5}	4.26×10^{-5}
K (km^{-1})	.0958	.1261	.1397
1/K (ft)	34,300	26,000	23,500
Γ (oK/km)	2.6	4.0	6.5
ρ_{tr} (slugs/ft^3)	1.915×10^{-3}	2.73×10^{-4}	7.07×10^{-4}
H_{tr} (km)	31.5	21.0	11.0
H entry (km)	250	165	161
ρ entry	3×10^{-12}	3×10^{-12}	3×10^{-12}
T_{iso}	86°K	86°K	217°K

CHAPTER 2

GENERAL ENTRY DYNAMICS

2.1 Introduction

Since the purpose of this thesis is to investigate design parameters for an unsophisticated probe to Jupiter for atmospheric determination, only trajectories which lend themselves to little or no guidance will be considered. This will limit us to a steep ballistic entry from deep space, a shallow entry from a disturbed reconnaissance orbit, or a decaying orbital entry. The use of a lifting vehicle will be prohibited by the delicate guidance required for orientation and attitude control. This first probe should be more like a meteor or bomb, and may broadcast only two things; stagnation point temperature and specific force. It may have to withstand specific forces up to 9000 Earth "g's", and will have to be dense enough to make a deep penetration before burning. It will use a thick ablative heat shield, and may rotate slowly to distribute heat evenly. It will contain no gyros or guidance system, and its transmitter will be potted solid state electronics and batteries.

In all these one pass ballistic entries, the specific forces (deceleration) will be far greater than the gravitational forces on the vehicle, and therefore the entry can be considered a

straight line. A further assumption is made of planar motion. Since Jupiter rotates so fast, the orientation of this plane will be important. However, it should be relatively easy to make the entry near the equatorial plane, and in the direction of rotation. This will considerably reduce the entry velocity with respect to the atmosphere.

The general three dimensional equations of motion for variable mass; oblate, rotating planet; and atmosphere with winds are spelled out in Duncan's thesis (ref 6). These equations cannot be solved in closed form, and are too complicated to be useful in showing variations of the parameters in question. For a probe as straight-forward as this, the two dimensional, constant mass, spherical rotating planet without winds will be entirely adequate. The vehicle is essentially a cannonball, and contains no guidance to utilize such nice refinements in motion.

The ballistics used will be those of Chapman (ref 7), and the modifications of Duncan (ref 6). Duncan's "conservation parameter" will not be necessary, since only the gas-dynamic phase is considered. The Keplerian and intermediate phases are of use only for guidance in the range of 10^{-4} to 10^{-2} "g's", and do not affect vehicle design for the final phase.

2.2 Types of Entry

The direct entry will be made at some entry angle, γ_b, from deep space with initial velocity, $v_i \doteq v_{esc}$. For Jupiter this would be about 200,000 ft/sec. But if the entry were made in the direction of planetary rotation, this value would be reduced by 41,000 $\cos \gamma_b$ ft/sec. This type entry requires no rocket thrust, and no

guidance other than the initial aiming.

The shallow entry would be accomplished by an impulsive perturbation from a stable reconnaissance orbit around Jupiter. The angle would be very shallow because large impulsive perturbations would require too much propellant. A reasonable value for γ_b would be 5°. The entry velocity would be on the order of satellite velocity, and could be reduced by almost the entire rotational velocity of the planet. Therefore $V_i \doteq 100{,}000$ ft./sec. This entry would be gentler than the first type, but would require a higher ideal velocity capability for the launching vehicle, and much more accurate guidance. Extra fuel would be required to establish the orbit, and still more to launch the probe from the orbit.

The orbital decay entry would be the gentlest possible without using a lifting vehicle, but it is also the most difficult to obtain. A low orbit within the sensible atmosphere would have to be attained, and would require the most careful guidance. The time required for this entry is longer than the others, as several passes around the planet would be made. The entry speed would also be about 100,000 ft/sec. and the maximum specific force would be 40 Earth g's. This shows that a lifting vehicle of some sort will certainly be required if a manned entry is ever made.

At the present time, the only entry available is the direct ballistic entry. But as we shall show, this would not be too hard to design with present materials, and would probably give the most useful information.

Equations will be included for instrumentation of the probe

in both flight path axes and energy axes. Flight path axes can be used regardless of the shape or orientation of the vehicle. The assumption has been made that for a steep entry the specific force lies along the flight path (Drag). Therefore, pendulous mounted instruments will indicate flight path axes even in a spherical rotating vehicle. Energy axes (r, ϕ) can only be used, however, in conjunction with a vertical indicating system. The resolution of the motion into radial and tangential components requires the angle γ_b. It is expected that such a system will not be included due to its complexity and delicate nature.

It should be emphasized that this instrumentation is to determine deceleration forces for radio relay, and is not intended for guidance. In this matter, small angle approximation and neglect of gravitational terms is allowed.

2.3 The Coordinate Frames

Figure 3 illustrates the two simple two dimensional coordinate frames used in the analysis. The r, ϕ, ψ frame is a great circle, planet centered frame which rotates with the vehicle. It can be considered an air mass frame or energy frame, as potential energy and angular momentum can be written in terms of r and ϕ. The entry trajectory is assumed to lie entirely in the r,ϕ plane; and the angle of this plane with the equator, ψ, is assumed to be small.

The flight path coordinates (x,z) are in the plane of r,ϕ and are rotated through the angle, γ_b.

2.4 The General Entry Equations

Accelerations:

$$A_r = \ddot{R} - \frac{V^2_I}{R} \qquad A_\phi = \dot{V}_I + \left(\frac{\dot{R}}{R}\right) V_{I\phi} \qquad (2\text{-}1)$$

Components of $V_{I\phi}$:

$$V_{I\phi} = V_{\phi} + W_{IJ} R \cos\psi = V \cos\gamma_b + W_{IJ} R \cos\psi \qquad (2\text{-}2)$$

where v = vel. with respect to the air mass,

and ψ = inclination of the trajectory plane with respect to the equatorial plane.

$$\dot{R} = V \sin\gamma_b \qquad (2\text{-}3)$$

It is useful also to define coordinates along and normal to the velocity vector as an x,z frame. (See Fig 3.) The x,z frame is rotated from the r,ϕ frame by the angle γ_b.

In x,z frame:

$$A_x = \dot{V} - W^2_{IJ} R \cos^2\psi \sin\gamma_b \qquad (2\text{-}4)$$

$$A_z = V\dot{\gamma}_b - \frac{V^2 \cos\gamma_b}{R} - W^2_{IJ} R \cos^2\psi \cos\gamma_b - 2W_{IJ} V \cos\psi$$

The forces to be considered are the gravitational forces and the drag force.

$$\bar{G} \doteq - G_{sp} \bar{l}_r$$

$$= - G_{sp}(\sin\gamma_b \bar{l}_x + \cos\gamma_b \bar{l}_z) \qquad (2\text{-}5)$$

and drag:

$$\bar{F}_D = - \frac{D}{M} \bar{l}_x \qquad (2\text{-}6)$$

Therefore the two dimensional equations of motion in the x,z plane are:

$$\dot{V} + (G_{sp} - W^2_{IJ} R \cos^2\psi) \sin\gamma_b + \frac{D}{M} = 0 \quad \text{(x force)} \qquad (2\text{-}7)$$

$$V\dot{\gamma}_b - \frac{V^2 \cos\gamma_b}{R} + (G_{sp} - W^2_{IJ} R \cos^2\psi) \cos\gamma_b - 2 VW_{IJ} \cos\psi = 0 \quad \text{(z force)}$$

Now, in dimensionless form, normalizing with respect to R_J, V_{sat}, $\frac{V_{sat}}{R_J} t$:

$$\frac{dv}{d\tau} + \left(\frac{1}{r^2} - r\Omega^2 \cos^2\psi\right) \sin\gamma_b + N_D = 0 \qquad (2\text{-}8)$$

$$v \frac{d\gamma_b}{d\tau} - \frac{v^2}{r} \cos\gamma_b + \left(\frac{1}{r^2} - r\Omega^2 \cos^2\psi\right) \cos\gamma_b - 2v\Omega\cos\psi = 0$$

In r, ϕ coordinates:

$$\frac{dv_r}{d\tau} - \frac{v_\phi^2}{r} + N_D \sin\gamma_b + \left(\frac{1}{r^2} - r\Omega^2 \cos^2\psi\right) - 2v_\phi \Omega\cos\psi = 0 \qquad (2\text{-}9)$$

$$\frac{dv}{d\tau} + \frac{v_\phi v_r}{r} + N_D \cos\gamma_b + 2v_r \Omega \cos\psi = 0$$

These equations can also be written in terms of energy and angular momentum, rather than coordinate forces. Defining zero potential energy with respect to Jupiter's gravitational field as the energy at infinity, total energy will be negative.

$$\frac{\mathcal{E}(tot)}{M} = - G_{sp} R + \frac{V^2 I}{2} \qquad (2\text{-}10)$$

In dimensionless form:

$$E_{(tot)} = \frac{\mathcal{E}(tot)}{MV^2_{sat}} = \frac{V^2 I}{2} - \frac{1}{r} \qquad (2\text{-}11)$$

Equating $\frac{dE}{d\tau}$ to power:

$$\frac{dE}{d\tau} = \bar{f} \cdot \bar{v}_I \qquad (2\text{-}12)$$

where $\bar{f}$ = the sum of all external forces in mean surface g's of Jupiter (dimensionless). This means of expressing motion is best for instrumentation, because accelerometers mounted within the body

can then measure the aerodynamic forces.

$$\frac{dE}{d\tau} = v_{I_r} \text{ (the output of the accelerometer in the } \bar{l}_r \text{ direction)} + v_I \text{ (the output of the accelerometer in the } \bar{l}_\phi \text{ direction).} \qquad (2\text{-}13)$$

If the body has aerodynamic stability, more useful information would come from body fixed axes.

$$\frac{dE}{d\tau} = v_{I_x} \text{ (output of accelerometer parallel to V)} + v_I \text{ (output of accelerometer normal to V)} \qquad (2\text{-}14)$$

The angular momentum of the vehicle about Jupiter provides the remaining energy expression needed.

$$P = RV_{I_\phi}$$

non-dimensionalizing: $p = \dfrac{P}{R_J V_{sat}}$

$$= r\,(v_\phi + r\Omega \cos \Psi) \qquad (2\text{-}15)$$

$$\frac{d\bar{p}}{d\tau} = \bar{r} \times \bar{f} \doteq r \text{ (accelerometer output in direction } \bar{l}_\phi) \qquad (2\text{-}16)$$

If r can be measured by radar or integrated from other data, the equations of motion can be written in energy and angular momentum form:

$$\frac{dE}{d\tau} = \frac{d}{d\tau}\left(\frac{v_I^2}{2} - \frac{1}{r}\right)$$

$$= (N_D)(v + r\Omega \cos \gamma_b \cos \Psi) \qquad \text{(energy)}$$

$$\frac{dp}{d\tau} = - rN_D \cos \gamma_b \text{ (angular momentum)} \qquad (2\text{-}17)$$

However, to utilize this system of instrumentation, the vertical will have to be known to provide the angle, γ_b; and to establish

the r,ϕ coord. system model. We note that it need not be an accurate vertical as would be necessary for inertial navigation, but only an approximation to the angle, γ_b. This could be obtained from an "albedo tracker", or perhaps some other form of optical or magnetic device.

Since refined measurements of forces are not needed, it is anticipated that the following data will be radioed back to Earth:

1) The drag load factor, N_D, which is the output of a pendulously mounted accelerometer within the vehicle.
2) The surface or internal temperature, or if the vehicle does not rotate, the stagnation point temperature.

2.5 General Solutions for Ballistic Entry

These solutions are all in non-dimensional parameters as defined in Appendix I. They are based on Duncan's approximations to Chapman's Z function analysis. Limits to the validity of each equation are stated with the equation.

The basic assumption in the ballistic entry is that γ_b is constant. That is, the drag specific forces are much greater than the gravitational forces. This assumption is valid for velocities above 25,000 ft/sec in the vicinity of Jupiter, and for γ_b such that:

$$k^{1/2}\gamma_b \geq 2.5 \qquad (2\text{-}18)$$

For Jupiter, this means an angle greater than approximately 2.3°.

$$\frac{dh}{d\tau} = - v \sin \gamma_b \qquad (2\text{-}19)$$

$$\frac{d\sigma}{d\tau} = \frac{d\sigma}{dh}\frac{dh}{d\tau} = - kv\sigma \sin \gamma_b \qquad (2\text{-}20)$$

The non-dimensional drag load factor, N_D, is defined as:

$$N_D = -\frac{dv}{d\tau} = \frac{1}{2}\rho_o R_J \frac{C_D S}{M}\sigma v^2 \qquad (2\text{-}21)$$

Therefore,

$$\frac{dv}{d\sigma} = \frac{dv}{d\tau}\frac{d\tau}{d\sigma} = \frac{1}{2}\frac{\rho_o R}{k \sin\gamma_b}\frac{C_D S}{M} v \qquad (2\text{-}22)$$

Separating variables and integrating, we have velocity as a function of density ratio, and atmospheric and vehicle parameters:

$$\ln\frac{v}{v_i} = \frac{1}{2}\frac{\rho_o R}{k \sin\gamma_b}\frac{C_D S}{M}(\sigma - \sigma_i) \qquad (2\text{-}23)$$

Range angle in the ballistic entry is found by the approximation:

$$X_N - X_i = \cot\gamma_b \ln\frac{r}{r_i} \doteq \cot\gamma_b (h - h_i) \qquad (2\text{-}24)$$

It has been assumed in the first chapter that:

$$\sigma = e^{-kh} \qquad (2\text{-}25)$$

All these solutions for altitude, density, and velocity can be written in terms of each other, or in terms of dimensionless time, τ.

Density ratio as the independent variable:

1) $h(\sigma) = -(\frac{1}{k}) \ln\sigma$ (2-26)

2) $v(\sigma) = v_i e^{(\frac{\rho_o R}{2k \sin\gamma_b}\frac{C_D S}{M})(\sigma - \sigma_i)}$ (2-27)

Altitude as the independent variable:

1) $\sigma(h) = e^{-kh}$ (2-25)

2) $v(h) = v_i e^{(\frac{\rho_o R}{2k \sin\gamma_b}\frac{C_D S}{M})(e^{-kh} - e^{-kh_i})}$ (2-28)

Velocity as the independent variable:

1) $\sigma(v) = \frac{2k \sin\gamma_b M}{\rho_o R \ C_D S}\ln(\frac{v}{v_i}) + \sigma_i$ (2-29)

$$2)\quad h(v) = -\frac{1}{k}\ln\left[\frac{2k\sin\gamma_b M}{\rho_o R C_D S}\ln\left(\frac{v}{v_i}\right) + e^{-kh_i}\right] \qquad (2\text{-}30)$$

Dimensionless time as the independent variable:

$$1)\quad \sigma(\tau):$$

$$-kv_i \sin\gamma_b\left[e^{-\left(\frac{\rho_o R C_D S\sigma_i}{2K\sin\gamma_b M}\right)}\right](\tau - \tau_i) = \ln\left|\frac{\sigma}{\sigma_i}\right| + \sum_{n=1}^{\infty}\left(-\frac{\rho_o R C_D S}{2k\sin\gamma_b M}\right)^n \left(\frac{\sigma^n - \sigma_i^n}{n\cdot n!}\right) \qquad (2\text{-}31)$$

$$2)\quad h(\tau):$$

$$-(\tau-\tau_i)kv_i\sin\gamma_b e^{-\left(\frac{\rho_o R C_D S}{2k\sin\gamma_b M}e^{-kh_i}\right)} = k(h_i - h) + \sum_{n=1}^{\infty}\left(-\frac{\rho_o R C_D S}{2k\sin\gamma_b M}\right)^n \left(\frac{e^{-nkh} - e^{-nkh_i}}{n\cdot n!}\right) \qquad (2\text{-}32)$$

$$3)\quad v(\tau):$$

$$-(\tau-\tau_i)kv_i\sin\gamma_b e^{-\frac{\rho_o R C_D S}{2k\sin\gamma_b M}\sigma_i} = \ln\left|\frac{2k\sin\gamma_b M}{\rho_o C_D S R\sigma_i}\ln\left(\frac{v}{v_i}\right) + 1\right| + \sum_{n=1}^{\infty}\frac{\left(-\ln\frac{v}{v_i}\right)^n}{n\cdot n!} \qquad (2\text{-}33)$$

The summation terms in the functions are the remaining terms from the series approximation to the exponentials, and may be dropped at the user's discretion.

We note that the vehicle parameter, $M/C_D S$, turns up in every equation, as well as the atmospheric parameter, $\rho_o R_J/2k$, and the entry angle γ_b. Specific solutions of the equations of motion for an entry into Jupiter are presented in the next chapter. These solutions will show the variation of the design parameters for

specific atmospheric parameters and entry angles.

2.6 Solutions for Specific Force and Stagnation Temperature

The two greatest problems in planetary entry are the high specific forces and heating encountered.

The specific force for a lifting vehicle at high Mach is expressed in non-dimensional form as:

$$f_E = \frac{G_J}{G_E} v^2 \frac{\rho_o R C_D S}{2M} \sigma \left[1 + \left(\frac{L}{D}\right)^2\right]^{1/2} \qquad (2\text{-}34)$$

This, in turn, can be expressed as a function of any other variable by using the equations in section 2.5. For example, as a function of velocity for a non-lifting body:

$$f_E(v) = \frac{G_J}{G_E} v^2 \frac{\rho_o R C_D S}{2M} \left[\sigma_i + \frac{2k \sin\gamma_b M}{\rho_o R C_D S} \ln \frac{v}{v_i}\right] \qquad (2\text{-}35)$$

This expression is in Earth "g's", and is valid when $\sigma_i << \sigma$. This function will have a maximum when:

$$\frac{d}{d\tau}(v^2\sigma) = 0$$

thus

$$\frac{dv}{d\tau} = \frac{kv^2}{2} \sin\gamma_b$$

and

$$v\,(f_E \text{ max.}) = .607 v_i \qquad (2\text{-}36)$$

This result is independent of vehicle parameters. The expression for maximum specific force depends on atmospheric and entry parameters only.

$$f_E(\max) = \frac{dv}{d\tau}(\max) = \frac{k(.607\ v_i)^2}{2} \sin\gamma_b \qquad (2\text{-}37)$$

The height at which this maximum N_D occurs, however, is a function of the vehicle design parameter, M/C_DS.

There are several heating factors of interest, but the stagnation point temperature will be the hottest to contend with. Also, the velocity at which the maximum stagnation point temperature is reached is independent of atmosphere and vehicle parameters.

$$T_s = 1.392 \times 10^4 \, (HF)_{EJ}^{1/4} \, (VF)^{1/4} \, (v^6\sigma)^{1/8} \, {}^oR \qquad (2\text{-}38)$$

$$\text{where "vehicle function" } (VF) = \frac{1}{K_{rad}\sqrt{RC}} \qquad (2\text{-}39)$$

and "heating function" is an atmospheric constant relating Jupiter to the Earth as follows:

ratios of:

$$(\mu)^{1/2}(G)^{3/2}(R)^{5/4}(K)^{1/4}(Pr)^{-2/3}\left(\frac{\frac{\gamma_J - 1}{\gamma_J}}{\frac{\gamma_E - 1}{\gamma_E}}\right)^{1/4} Z^{1/2} \qquad (2\text{-}40)$$

The value of this heating function for Jupiter is about 64.2. This will be discussed more fully in the next chapter.

The stagnation temperature as a function of velocity is:

$$T_s\,(v) = 1.392 \times 10^4 \, (HF)_{EJ}^{1/4} \, (VF)^{1/4} \, \left(\frac{2k \sin\gamma_6 M}{\rho_o R C_D S} v^6 \ln \frac{v}{v_i}\right)^{1/8} \qquad (2\text{-}41)$$

This is a maximum when $\frac{d}{d\tau}(v^6\sigma) = 0$

$$\frac{dv}{d\tau} \quad \frac{kv^2 \sin\gamma_6}{6}$$

$$\text{and} \quad v(T_s \text{ max.}) = .846 \, v_i \qquad (2\text{-}42)$$

Use will be made of these factors, to show where maximum specific force and temperature are expected, in the velocity vs. altitude plots in the next chapter.

Little has been said of the decaying orbital trajectory. Such an entry would require an extreme accuracy in guidance, beyond the scope of this simple probe. The escape from Earth and establishment of a reasonable transfer ellipse (2 yr 9 mo.) requires an ideal velocity potential of about 14.3 km/sec (ref 5). To establish a stable orbit about Jupiter at all will require an additional ideal velocity of 5.7 km/sec. This would be taxing the present level of rocketry to its limit. A totally rocket braked soft landing would require 66 km/sec. more, and is out of the question.

The equations for establishing a decaying orbit are outlined in Duncan (ref 6). There is first the circularization phase during partial passes through the atmosphere; then the decay phase. These equations are non-linear, and have not been solved in closed form. However, machine solutions give a maximum N_D for Jupiter of 40 Earth g's, and a stagnation point temperature of 2.7 times that for entry into Earth (ref 7). It appears that the unmanned entry is possible, but the establishment of the necessary low orbit is beyond the state of the art in guidance. We will therefore concentrate on the unguided ballistic entry.

CHAPTER 3

BALLISTIC ENTRY INTO JUPITER

3.1 Introduction

This chapter deals with the specific entry profiles into Jupiter. Solutions to the equations presented in the second chapter are calculated for entry into the two model atmospheres. For each atmosphere, and for several entry angles and velocities, velocity profiles are calculated. These show a variation with the vehicle design parameter, $M/C_D S$.

Also developed here are specific force and heating profiles. The heating problem will be considered in two phases:

1) Total heat absorption, Q_T.

2) Maximum heating rate, $\dot{Q}_{max}$.

Preliminary calculations have shown a range in the vehicle design parameter from 4 to 100 slugs/ft.^{2}, and these values are included in the figures. Finally, with an eye toward instrumentation, specific force and stagnation heating rate plots against real time are generated. These vary with design parameter, atmosphere model, and entry conditions, and are the predictions upon which experimental atmospheric determination is suggested.

3.2 Velocity vs. Altitude

The expression as developed in chapter two is calculated here:

$$v(h) = v_i e^{\left(\frac{\rho_o R C_D S}{2k \sin\gamma_b M}\right)(e^{-kh} - e^{-kh_i})} \qquad (3\text{-}1)$$

The plots are made as a ratio of v/v_i against altitude, H. Therefore, an entry from any initial velocity can be considered from these graphs. The initial conditions vary with the model atmosphere as follows:

1) Model a, Figures 5a, b, c

   a) $\rho_o = .0082$ slugs/ft.^{3}

   b) $k = KR_J$

      $= 7615$

   c) $M/C_DS = 4$ to 100 slugs/ft.^{2}

   d) $\gamma_b = -5°, -30°, -60°$

   e) $h_i = H_i/R_J$

      $= .003$ ($H_i = 500{,}000$ ft.)

2) Model b, Figures 4a, b, c

   a) $\rho_o = .0009$ slugs/ft.^{3}

   b) $k = 8840$

   c) $M/C_DS = 4$ to 100 slugs/ft.^{2}

   d) $\gamma_b = -5°, -30°, -60°$

   e) $h_i = .002$ ($H_i = 333{,}000$ ft.)

The values of γ_b were chosen as representative of the direct entry, and also the disturbed orbital entry. As previously stated, an economical use of mass ratio will only allow the $\gamma_b = -5°$ case for disturbed orbital entry. These solutions are valid to about .25 v_i. Beyond this point, gravitational forces are significant, and changes in C_D and other parameters are apparent as Mach number falls below about ten. However, the

profiles cover the range in which heating and deceleration effects are greatest, and will therefore be useful. These solutions were compared to sample calculations by machine from Chapman (ref 7), and agree closely with the more accurate solutions obtained there.

The most significant finding here is that an extremely dense vehicle will be required to reach the cloud layer, if model "a" is accepted. Even at $\gamma_b = -60°$, $M/C_D S$ must be 100 to arrive at the cloud layer while still in the entry phase. If we wish to ascertain the properties of this cloud deck, we must arrive there while there is still a clean cut response from either the heating rate or specific force measurements. This is easily accomplished in the model "b" atmosphere.

3.3 Specific Force

The specific force in earth g's has been given in chapter two as:

$$f_E(v) = \frac{G_J}{G_E} \frac{\rho_o R C_D S}{2M} v^2 \left(\sigma_i + \frac{2k \sin \gamma_b M}{\rho_o R C_D S} \ln \frac{v}{v_i}\right) \qquad (2\text{-}35)$$

This force is assumed to be all along the flight path over the portion of the trajectory where G is not considered. In addition, if we consider v_i as entry velocity, and σ_i as negligible, the maximum specific force is <u>independent of vehicle design</u>. Thus the non-dimensional drag load factor is given by:

$$N_D(v) = \frac{G_J}{G_E} k \sin \gamma_b \, v^2 \ln \frac{v}{v_i} \qquad (3\text{-}2)$$

This load factor is a function of entry angle, entry velocity, and present velocity. Present velocity, as a function of height, is also a function of vehicle design. The <u>maximum</u> load factor, however, is a function only of the atmosphere, entry angle, and entry velocity.

The entry velocity relative to the air mass is in turn a function of entry angle and planetary rotation. In the case of the Terrestrial planets, the rotation is negligible. But Jupiter's large radius and fast rotation period (9 hours, 50 minutes), make inclusion of rotation velocity necessary. Figure 6 shows a plot for both atmospheres of N_D vs entry angle considering rotation for the direct entry. Jupiter's equator lies nearly in the ecliptic plane, and we assume a probe will remain in the ecliptic plane for minimum energy requirements. Therefore, a range of 180° in entry angle along the equator is covered, considering the preferred entry with the rotation, and the disastrous one against the rotation. The graph clearly shows the effect of the rotational velocity of 41,000 ft/sec.

We note with some concern that for the usual entry, atmosphere b with the rotation, we can expect 100 earth g's per degree of entry angle! Specially constructed vacuum tubes can take about 400 g's. Therefore we must limit the probe to 4° entry angle if we use a vacuum tube transmitter. This limit is too restrictive on the guidance system, and we will have to use solid state electronics capable of about 3000 g's for a 30-degree entry.

Accelerometers are available to measure N_D up to 10,000 g's (piezo-electric accelerometers). The accelerometer system and its two gimbal mount with four roller bearings will be designed for 10,000 g's. We note for interest that for a .1 pound accelerometer, the outer gimbal bearings will be freight car type roller bearings with 50,000 pound capacity each.

For a disturbed orbital entry, the maximum N_D expected is

shown in Figure 7. Here the entry angle is more easily controlled, and the entry velocity is lower. The expected N_D is 40 g's per degree entry angle. Also, because of fuel limitations, a maximum entry angle of five to seven degrees is expected. The vehicle could then use vacuum tube electronics, and be designed for 250 g's. But all this relief comes at great expense when it is realized that the vehicle must first be put into a stable orbit about Jupiter. Also, we see from recent experience with the Discoverer satellite series, that firing a retro-rocket by remote control is largely unsuccessful.

The variation in specific force with altitude was calculated, and plotted in Figure 8. This graph shows how the vehicle design parameter controls the height for maximum N_D. There are plots for the several entry angles used as examples for parabolic and orbital decay entries. This information can be used to determine the N_D vs time profile for the selected design. It represents dv/dt vs H, and therefore H vs time can be derived. It is rather too much work to derive this for every possible case, but it will be done for the design chosen in the next chapter. The specific force variation with time will be one of the transmitted outputs.

Figure 9 is an illustration of the time profiles to be expected. All quantities are specified, and the results in N_D, H, and V are plotted. We see here that the entry phase is very short compared to an entry into Earth. The deceleration phase takes approximately three minutes for Earth, while it only lasts 15 seconds for Jupiter. This short time will aid us in the structural considerations for design.

3.4 Heating

The expected heat generation profiles will be calculated here.

The problem of handling the heat will be considered with the vehicle design. Most sources agree that for a ballistic entry, re-radiation of heat is insignificant. These people are thinking in terms of an Earth entry of about three minutes duration. For the Jupiter entry of 15 seconds duration, there will be even less chance of a radiative equilibrium. We will, therefore, only consider the convective terms in the heat flow equations as presented by Chapman and Duncan.

This convective heat will occur almost entirely in the continuum flow regime. According to the Blasius boundary layer equation, the heat transfer through a laminar boundary layer is inversely proportional to the square root of the local Reynolds number based on the radius of curvature of the nose. Thus, for bodies in the same environment, the heat input rate per unit area and time will be inversely proportional to the square root of the radius curvature of the missile nose.

In the ablative heat shield case, a sharp nosed body would soon be reduced to a blunt nosed body due to the small amount of ablative material in the pointed portion of the missile. The primary reason for using a blunt body is to secure the high C_D necessary for deceleration at high altitude.

The stagnation point convective heat rate is given by the expression:

$$(\dot{Q}_c)_s = \frac{C_{atm}}{\sqrt{RC}} \left(\frac{\rho}{\rho_o}\right)^n \left(\frac{V}{\sqrt{GR}}\right)^m \frac{BTU}{ft^2\text{-sec}} \qquad (3\text{-}3)$$

C_{atm} is a function of the atmosphere, and is given as 18,000 for Earth, and works out to 1,590,000 for model b and 4,750,000 for

model a. Compared to Earth, the heating rate will be 87 and 264 times worse, respectively.

In terms of our non-dimensional parameters, the heating rate:

$$\dot{Q}_s = \frac{C_{atm}}{\sqrt{RC}} (\sigma)^n (v)^m \frac{BTU}{ft^2\text{-sec}} \qquad (3\text{-}4)$$

The exponents on density ratio and velocity ratio depend on the flow conditions in the boundary layer. This in turn depends on the Reynolds number.

For laminar flow, where μ is proportional to $\sqrt{T}$, then $n = 1/2$ and $m \doteq 3$.

For turbulent flow, $n \doteq .8$ and $m \doteq 2.2$ (from Chapman). Figure 10 is a plot of Reynolds number at maximum stagnation temperature velocity ($.846\ v_i$) for various M/C_DS ratios. Chapman states that we can have high hopes of maintaining laminar flow in the boundary layer. But this plot shows that laminar flow can hardly be expected over much more than one foot of the Jupiter probe vehicle. If we assume the boundary layer will become turbulent at 6 or 7 million, a body of $M/C_DS = 10$ at an entry angle of 30 degrees will have laminar flow for about one foot from its leading edge. However, if the body is blunt enough (e.g., like a Mercury Capsule) most of the heating will occur over the laminar flow regime.

These extremely blunt bodies will suffer more from radiation heating from the hot gas to the vehicle, but the time of flight is so short we believe radiation will have little effect on the total heating problem.

The maximum laminar heating rate is given by the expression:

$$(\dot{Q}_c)_s\ (max) = \frac{C_{atm}}{\sqrt{RC}} (.605) (\sigma)^{1/2} (v_i)^3 \qquad (3\text{-}5)$$

This is a function of M/C_DS and entry conditions. The density ratio used is that for which $v = .846\ v_i$, and is calculated from the graphs in Figures 4 and 5. Figure 11 is a plot of the maximum laminar stagnation point heating rate expected vs. the design parameter M/C_DS. Also shown on this graph for comparison are the maximum allowable heating rates for Teflon and graphite ablative heat shields on a spherical vehicle (ref 8,9). This graph indicates at once that we will not be able to tolerate steep ballistic entries with our present ablative protection. This is one of the important constraints to be used in the next chapter.

Figure 12 is an example of a heat rate vs. time plot for a particular entry configuration. The integral of plots such as these will give the total heat absorbed, and will determine the weight of ablative material to be used in the vehicle design.

3.5 Summary

We have now developed particular constraints for the Jupiter probe. The structural limitations under high specific force, and the heat dissipation problem will determine the upper limit of severity of the entry. Fortunately, human factors are not involved. The increase in guidance requirements, and mass ratio of the booster will determine the practical floor on the gentleness of the entry. In the next chapter, we shall see whether these constraints leave a channel of possibility for the Jupiter probe using present day hardware.

The heating rates developed here are for a laminar boundary layer. The heating rates in a turbulent boundary layer, due to better convection, would be prohibitive. But we must not fool

ourselves into thinking the boundary layer will remain laminar very far aft of the nose. This requirement on boundary layer will present a further constraint.

Stagnation point temperature, per se, has little relation to the entry profile when an ablative coating is used. The shield quickly heats to the vaporization temperature, and remains constant while the heat is dissipated. This boiling off of the gaseous material further shields the vehicle itself from convective heat input. The vehicle skin will remain below the critical 2000°F temperature (for steel) as long as the coating lasts. This is due primarily to the poor heat conduction of the ablative coating. These considerations will influence the instrumentation of the probe.

The problem of communication of the data back to Earth is not considered in this thesis. However, it should be recognized that an ionized shock layer may interfere with electromagnetic transmission at certain frequencies. The detail design of the antenna, and the selection of transmitting frequency, will have to include consideration of the degree of ionization in the atmosphere around the vehicle.

CHAPTER 4

CONSTRAINTS ON VEHICLE DESIGN AND FEASIBILITY OF ATMOSPHERIC DETERMINATION

4.1 Introduction

At this point, we must examine the constraints imposed on the vehicle design by the forces and heating rates calculated in the previous chapters. We will then estimate the constraints due to the present limitations in guidance. The vehicle configuration will be specified. Within the area of possibility for a successful entry, we will discuss the feasibility of atmospheric model determination. The conclusions and recommendations will follow.

4.2 Heating Rate Constraints

We have discovered that the only feasible means of heat dissipation will be an ablative shield. In view of this, and the short time duration of the heat input (2 to 10 seconds), the heating of the vehicle core should be acceptable. We can carry enough heat shield without a great payload penalty to handle even this large amount of heat. The vaporization of the material will not only carry away heat to the surrounding air, but will provide an insulating region of vaporized material to further shield the vehicle from heat convection. Despite the large heat inputs, the

materials used are poor conductors, and the interior should remain below its critical strength temperature (2000°F for steel).

The material most generally used for this type shield is Teflon (a Dupont trademark for polyethoflourethylene). It is a plastic with strength at high temperatures, and is easily molded. Its heat capacity to vaporize is about 10,000 BTU/lb., and the maximum heat rate input is about 50,000 BTU /ft.^{2}sec. (ref. 8). This limit keeps the material from boiling off so fast that it explodes.

The best material for an ablative heat shield from the point of view of heat capacity is graphite. Graphite can dissipate about 30,000 BTU/lbs., and at a rate of 150,000 BTU/ft.^{2}sec. But there are many structural problems associated with the use of graphite that have not yet been solved. It is brittle, and hard to cast unless it is mixed with other more plastic compounds. But such a mixture lowers the heat capacity. Perhaps a mixture of Teflon and graphite may be successfully used.

The heat rate input graph (Figure 11) shows the limits imposed by these materials on the type of possible entry. The Teflon coated sphere of reasonable density (from 1 to 4 with respect to water) can only be used for the deflected orbital entry. If we allow a solution to the graphite structural problem, we can still only make a 20 degree direct entry. These are the rather stringent constraints imposed by the maximum allowable heat rates.

4.3 Configuration

Another glance at Figure 11 shows us that the lighter vehicles will allow a steeper trajectory than the heavy ones. Most of the missiles used today have a payload specific weight very close to

one (with respect to water). Figure 13 shows the variation in M/C_DS with radius of curvature for a sphere. Figure 14 shows this information for a typical final booster stage, and Figure 15, for a project Mercury shaped capsule. A C_D of 1.0 is used for these shapes at hypersonic velocities. The Pioneer V probe has shown a deep space launching capability of about 100 pounds payload. The Saturn booster is reported to have a 15,000 pound payload. These lines are also indicated on the configuration graphs.

It is apparent that if we limit ourselves to 100 pounds, we can only attain M/C_DS of about 4 slugs/ft.^{2}. This would be to our advantage for heat protection, but would not allow penetration to the vicinity of the cloud level during the entry phase. Using the Saturn booster, we can attain M/C_DS on the order of 20 slugs/ft.^{2} This would give us the desired profile in atmosphere model b. We would have to go to still greater weights to reach the clouds for atmosphere model a.

We note that the project Mercury capsule has the advantage of a larger radius of curvature for its diameter than the other typical shapes considered. This shape has been demonstrated to have aerodynamic stability at high Mach number, but a still flatter nose would probably lead to instability. In Figure 15 we have run the calculations to a density of 7. This would be a solid steel vehicle with a graphite heat shield, and would approximate the limit of density in vehicle design.

In order to show variation of design to best advantage in terms of mission, entry angle, and M/C_DS we must assume some basic limits. We assume that the Saturn booster is available,

and that a graphite heat shield can be used. We therefore let the weight equal 15,000 pounds. We allow average vehicle density to run from 7 to 0.3 with respect to water. We limit the vehicle size to a 10-foot diameter.

Using these criteria, and satisfying the maximum heat rate constraint, we develop the plot in Figure 16. The variation of M/C_DS with entry angle as a function of vehicle average density for the three shapes chosen is shown. The mission requirement is arbitrarily set as reaching the clouds with $v = .25\ v_i$. From Figure 16, several facts are evident.

1) With the very low M/C_DS compatible with the present 100 pound launch capability, the vehicle cannot hope to reach low altitudes during the entry phase. We must therefore wait for the Saturn booster.

2) The conical shaped vehicle has an advantage due to its larger radius of curvature for a given vehicle diameter. This vehicle can come fairly close to meeting the mission requirement.

3) It would tax the imagination to conceive of a vehicle large enough to penetrate atmosphere model a to the cloud level. M/C_DS would have to be 100 slugs/ft.^{2}, and with a solid steel vehicle, the diameter would be 20 feet, and the weight would be 127,000 pounds. In addition, the ablative material would have to absorb 450,000 BTU/ft.^{2} sec.

4) There will be a lower limit on the vehicle average density dictated by the specific force requirements. A detailed structural analysis is beyond the scope of this thesis. The specific force goes up practically linearly with entry angle if we enter in the

direction of planetary rotation, and figures to about 100 Earth g's per degree. We suggest that a reasonable structural limit for a design load factor of 3000 would produce an average vehicle density of two.

5) It is evident from the figure that high M/C_DS alone does not guarantee a deep penetration. The heating rate constraint limits such dense vehicles to a low entry angle for parabolic entry velocity.

6) The deflected orbital entry is virtually free from heating constraints. Any of these vehicles with an M/C_DS of 100 can enter at more than 30° without overheating. But the deflected orbital entry is not that easily accomplished. We are limited by fuel carried in the vehicle to a deflection of 5 or 10 degrees. From Figure 16, we must have a high M/C_DS. At 5° deflection we must have 100 slugs/ft.^{2} Only the rocket shaped vehicle can reach that high an M/C_DS without exceeding the 15,000 pound weight limit.

The configuration chosen as most likely to succeed is the Mercury capsule shape with an average density of two. The entry angle should be near 30°. The M/C_DS is 11, the nose radius and vehicle diameter is 8.5 feet, and the weight is 15,000 pounds. A graphite heat shield is used, and the maximum heating rate will be 150,000 BTU/ft.^{2}sec. The significant heating period is 2.4 seconds, and by graphical integration the total heat absorbed is 180,000 BTU/ft.^{2} of heat shield (Figure 12). This specifies the shield weight as 6 pounds/ft.^{2} (Ref. 9), and makes total ablative material weight 1360 pounds, or about 9% of the vehicle weight. Other materials or cooling systems would require much greater

weight, and this 9% seems to be a practical low for the Jupiter entry vehicle. The interior will stay relatively cool as long as there is some of the ablative shield remaining. If we make the shield lighter, the structure would melt or lose strength as soon as the ablative material evaporates. The majority of the deceleration loads occur after the heating phase, and we must not allow the vehicle to become weakened early in the trajectory.

The heating protection described here is for the model b atmosphere. From Figure 11 it is evident that only a 5° entry could possibly be tolerated in atmosphere a. Such an entry would not meet mission requirements, or guidance constraints. It is only practical, then, to design the vehicle for model b, and allow its failure in model a to be an indication of the atmosphere.

4.4 Guidance Constraints

It is difficult to say just how good our present guidance systems are. The Pioneer V probe to the orbit of Venus was judged to have performed perfectly. Yet it is short of its goal by several thousand miles due to a booster burning time uncertainty of less than one second. It seems clear, then, for a precision injection at any controlled angle into Jupiter, we must have mid-course and terminal guidance. Such a system, furthermore, must operate automatically without signals from Earth. It must take its measurements in the vicinity of Jupiter from the fields of Jupiter (optical, magnetic, or electric). It would probably carry a model inertial reference frame (stable platform with gyros), which would be corrected for drift periodically by star trackers during its 2 year 9 month journey.

This system does not exist today, as far as the unclassified

literature is concerned. If it did, it would have been used in the Pioneer V probe to Venus. Such developments may reasonably be expected in the next ten years, however, The consensus at this Institute is that with our present launch guidance we would be lucky to hit Jupiter at all. The Keplerian trajectory and ballistic entry make no provision for corrections to launch errors, and certainly we could not expect a precise injection angle, much less a stable orbit about Jupiter.

It might be interesting to consider the statistical chances of attaining a 30° or less injection in the direction of planetary rotation, assuming we can attain a parabolic contact with the planet. This would be an academic study at best, for we must not expect the United States to expend this awful amount of money without a good probability for success. It seems we are constrained to wait for a system including terminal guidance.

4.5 Feasibility of Atmospheric Determination

For this discussion, we shall assume we can make the 30° entry with the vehicle selected under section 4.3. What information should we instrument and radio back to Earth?

An examination of Figure 6 indicates that there is considerable difference in the maximum specific force expected in the two atmospheres. Model a will present an N_D (max) 24% lower than model b. This difference is quite sensitive to entry angle, however, and an error of 10° in entry angle will also equal 24% of N_D. We must therefore include instrumentation to measure the entry angle. Even if this angle cannot be controlled, the model atmosphere can be ascertained if the angle and its degree of

certainty are known. The maximum specific force is a definite quantity not dependent on the vehicle configuration, and therefore not subject to uncertainties such as C_D, or effective drag area (which may be considerably larger than the cross sectional area of a vehicle in an ionized gas). This force is a function solely determined by the entry parameters (which we have assumed are successfully controlled), and the atmospheric parameter, k, to be determined.

The skin temperature or its derivative appear to hold atmospheric information for us also. Figure 10 shows that the Reynolds numbers for the two models are nearly identical. However, the heating profiles are quite different. The higher cloud level pressure and density of model a account for the higher heating rates (Figure 11). Unfortunately, a temperature would be difficult to instrument in a vehicle incorporating an ablative heat shield. The heating is wholly transient, and in the short effective heating period, no equilibrium temperatures are reached. Further, the temperature or heating rate are quite sensitive to uncertainties such as C_D, S, Prandtl number and viscosity. To use heating as a determinant, these instrumentation difficulties and uncertainties would have to be overcome.

A very useful determinant would be altitude, and its measurement by radar would also provide the entry angle γ_b, needed for N_D determination. The height at which maximum N_D occurs varies considerably with the atmospheric parameter (Figure 8). The clouds of Jupiter are expected to be ammonia cirrus (solid crystals), and would give a good radar echo to the proper frequency emission. The

radar could be made to track minimum range, and the dish angle would then be the flight path angle.

There would be difficulties with the radar, of course. The tracking mechanism would have to be perfectly balanced and very rugged to endure 3000 g's. The electronics would have to be all solid state. There may be interference, as with the radio transmission, from the ionized shock layer. But these problems are not insurmountable, and should require no more development time than the guidance system required.

Even without the radar, specific force measurements would be indicative of the atmosphere to the degree of uncertainty of the entry angle.

4.6 Conclusions and Recommendations

The major problem appears to be control of the entry angle. Atmospheric determination can be made if the entry is successful, and if the entry angle is known within about five degrees. To make a successful entry, the entry angle must be controlled to 30° or less.

The mission is stymied at present by the lack of a mid-course and terminal guidance system that would provide this accuracy in entry angle. Such a system is probably under development at this time. It need not be stressed for the high load factors encountered during the entry phase. It would be sufficient to control the entry angle prior to the onset of the specific forces.

If this controlled entry angle were reliable, the only instrumentation needed in the entry vehicle would be a pendulously mounted piezo-electric accelerometer. A potted electronics

transmitter could be built to broadcast the load factor thus measured. If the controlled entry were not reliable to within five degrees, a device would be needed in the probe to measure the actual angle. If radar is developed for this measurement, it can also supply the vehicle height above the clouds. This height can be used as a cross check in atmospheric determination.

The vehicle itself will have to be large. In the Mercury capsule configuration the vehicle could reach nearly to the cloud level at a weight of 15,000 pounds. This will require the Saturn booster for launch and a graphite heat shield -- both under development at this time. The present deep space launch capability of 100 pounds will not be adequate for the Jupiter probe. A Teflon heat shield does not have enough heat rate capacity for the direct entry, but would do for the deflected orbital entry.

The decaying orbital and deflected orbital entries are still farther into the future with respect to guidance.

The primary purpose of the mission is to determine the molecular weight of Jupiter's atmosphere. It has been shown that this can be done with a large, but simple, entry vehicle. But the entry vehicle must be delivered to the entry point by a much more sophisticated navigational vehicle. This delivery is beyond the present state of the art of guidance.

We suggest for further study the following points:

1) The detailed structural design of the vehicle to withstand the high load factors encountered;

2) The degree of ionization in the shock layer, and its effect on electro-magnetic transmission;

3) The chemical effect of the heat and the reducing atmosphere on the ablating material;

4) The probability of achieving a 30° or less entry angle with present day launch guidance only.

We believe the guidance, booster, and graphite heat shield problems are currently under consideration.

APPENDIX I

NOTATION AND SYMBOLS

A. Subscripts

γ, ϕ, ψ	Components along the $\bar{l}_\gamma$, $\bar{l}_\phi$, $\bar{l}_\psi$ axes.
i	Initial value of the quantity.
I	Measured with respect to inertial coordinates.
J	The quantity for Jupiter.
E	The quantity for Earth.
b	Refers to ballistic entry.
s	Refers to stagnation area.

B. Symbols

$\bar{A}$	Acceleration vector of entry vehicle, ft/sec^2.
C_{atm}	Dimensional constant for the planetary atmosphere. $(BTU\ ft^{-3/2}\ sec^{-1})$
C_D	Drag coefficient.
C_P	Heat capacity at constant pressure.
C_V	Heat capacity at constant volume.
D	Drag force (lb.).
$\mathcal{E}$	Energy (ft-lb).
E	Dimensionless energy $= \dfrac{\mathcal{E}}{MV^2_{sat}}$
$\bar{F}$	Specific force $(ft/sec.^2)$
$\bar{f}$	Dimensionless specific force in surface g's of the planet. $\bar{f} = \dfrac{\bar{F}}{G}$
$\bar{G}$	Gravitational field intensity (ft/sec^2)
$\bar{g}$	Planet's gravity field (ft/sec^2)
H	Altitude of vehicle above planetary reference level (ft).

h Dimensionless altitude = $\frac{H}{R}$

K Exponential decay parameter of planetary atmosphere (ft^{-1}).

K_{rad} Vehicle surface radiation emissivity.

k Dimensionless decay parameter of planetary atmosphere = KR

M Mass of vehicle (slugs)

M_J Mass of planet (Jupiter, in this case)

N_D Dimensionless drag load factor = $\frac{D}{MG}$

P Angular momentum per unit mass of the vehicle

p Dimensionless angular momentum = $\frac{P}{R^{3/2}\ G^{1/2}}$

P_r Prandtl number

Q_c Total convective heat absorbed per unit area. $(\frac{BTU}{ft^2})$

RC Radius of curvature of vehicle nose (ft).

R_g Universal gas constant = 8.31×10^7 ergs/°K

$\bar{R}$ Radius vector from planet center to vehicle

$\bar{r}$ Dimensionless radius vector = $\frac{\bar{R}}{R_J}$

Re Reynolds number = $\frac{\rho V \text{ length}}{\mu}$

S Reference area of entry vehicle used in drag computations (ft^2).

T Temperature (°K).

t Real time (sec).

$\bar{V}$ Velocity vector of a vehicle with respect to coordinates rotating with a planet.

v Dimensionless velocity = $\frac{V}{V_{sat}}$

V_{sat} Circular orbital velocity at planet surface = $\sqrt{GR}$

X Distance flown measured at surface of planet

Z Chapman's transformation variable = $\frac{v \cos \gamma_b \sin \gamma_b}{\Xi \sqrt{k}}$

C. Greek Symbols

γ Ratio of specific heats C_p/C_r

γ_b Ballistic entry angle

Γ Dry adiabatic lapse rate (°K/km)

μ Coefficient of viscosity of the planet's atmosphere (slugs/ft-sec)

ρ Free stream atmospheric density (slugs/ft^3)

ρ_o Reference level atmospheric density

σ Density ratio ρ/ρ_o

$\sum_{n=1}^{\infty} ( )_n$ Summation of quantities in parenthesis

τ Dimensionless time = $\frac{V_{sat}}{R} t$

ϕ Angle measured in plane of trajectory from a reference point in the direction of motion

ψ Angle of inclination of the trajectory plane with the planet's equatorial plane.

Ω Dimensionless angular velocity of the planet about its polar axis

$$\Omega = \omega_{IJ} \sqrt{\frac{R}{G}} \quad \text{for Jupiter}$$

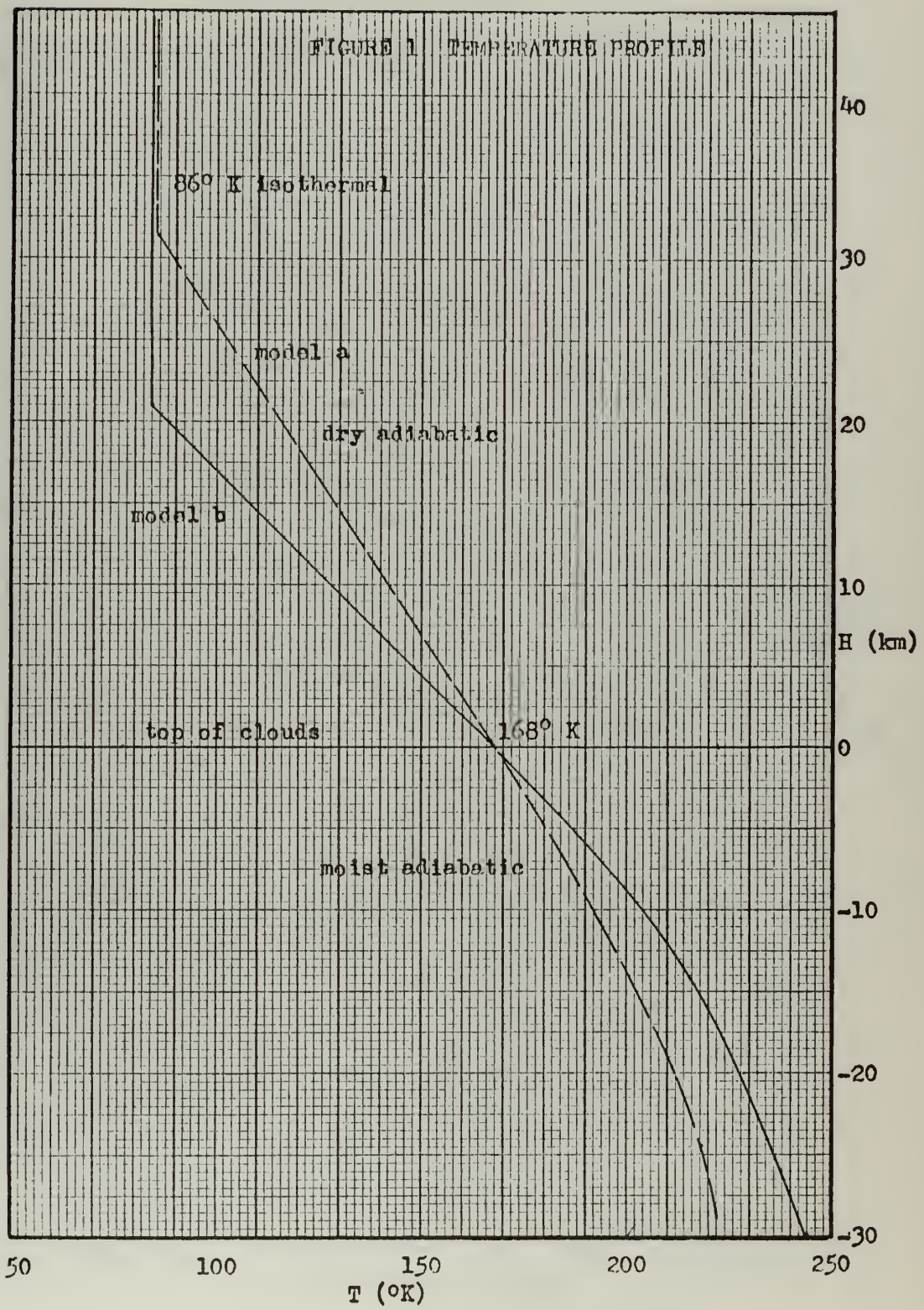
FIGURE 1 TEMPERATURE PROFILE
86° K isothermal
model a
dry adiabatic
model b
top of clouds
168° K
moist adiabatic
40
30
20
10
0
-10
-20
-30
H (km)
50
100
150
200
250
T (°K)

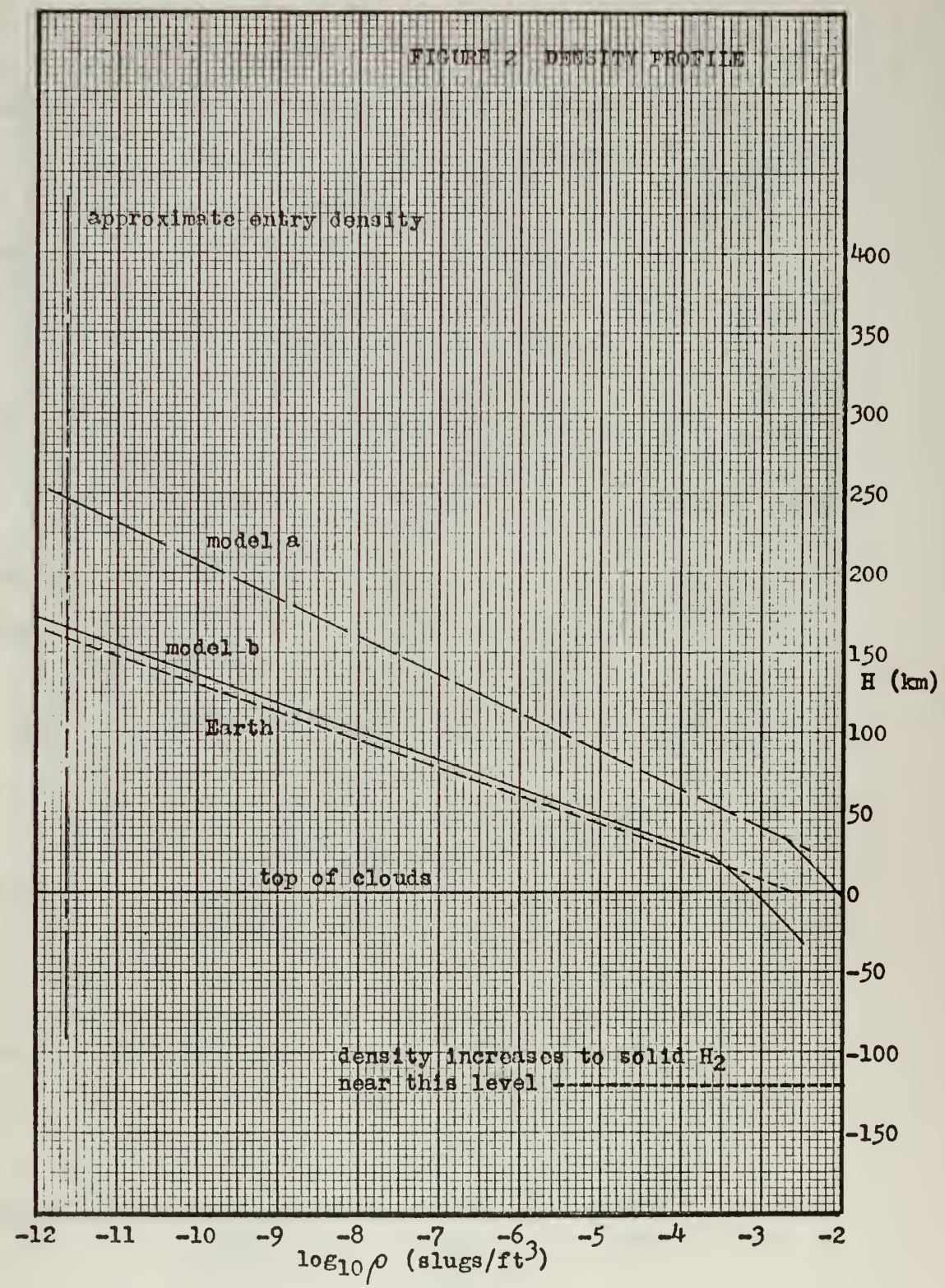
FIGURE 2 DENSITY PROFILE
approximate entry density
model a
model b
Earth
top of clouds
density increases to solid H_2
near this level
400
350
300
250
200
150
100
50
0
-50
-100
-150
H (km)
-12
-11
-10
-9
-8
-7
-6
-5
-4
-3
-2
$\log_{10}\rho$ (slugs/ft^3)

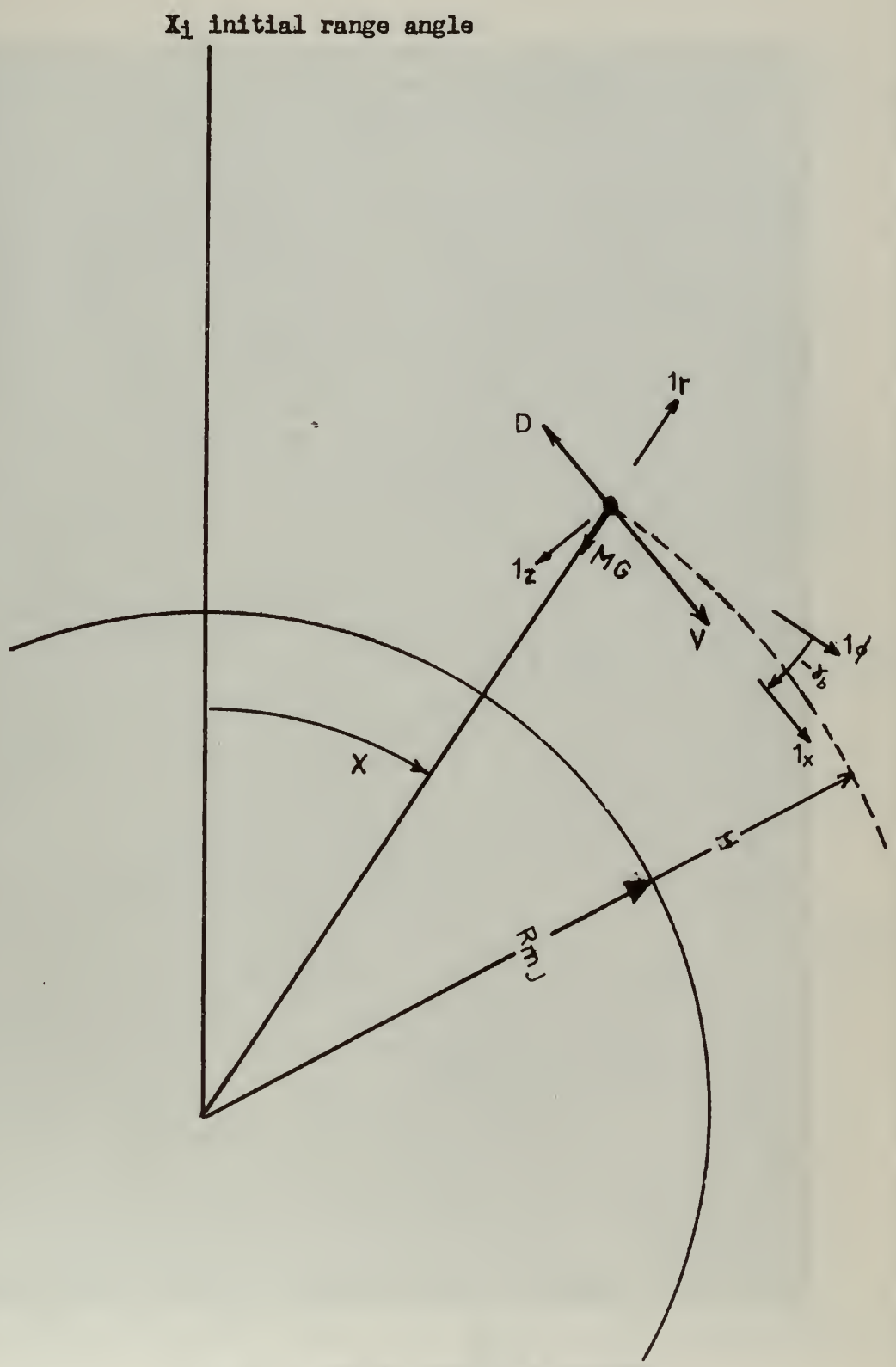

FIGURE 3 ENTRY COORDINATE SYSTEMS

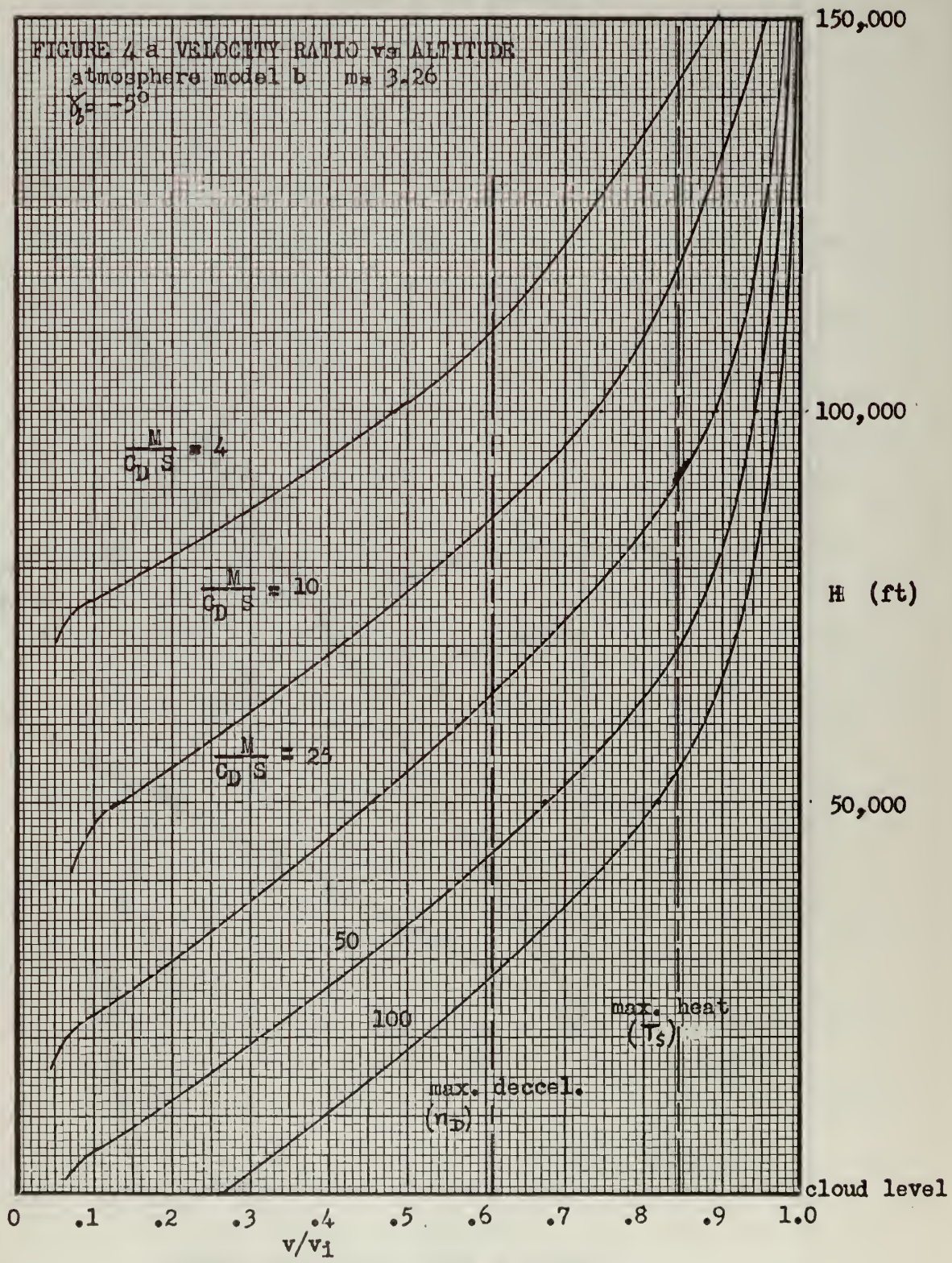
FIGURE 4 a VELOCITY RATIO vs ALTITUDE
atmosphere model b m= 3.26
$\gamma_b = -5^0$
$\frac{M}{C_D S} = 4$
$\frac{M}{C_D S} = 10$
$\frac{M}{C_D S} = 24$
50
100
max. heat
$(\dot{T}_s)$
max. deccel.
(n_D)
150,000
100,000
50,000
H (ft)
cloud level
0
.1
.2
.3
.4
.5
.6
.7
.8
.9
1.0
v/v_i

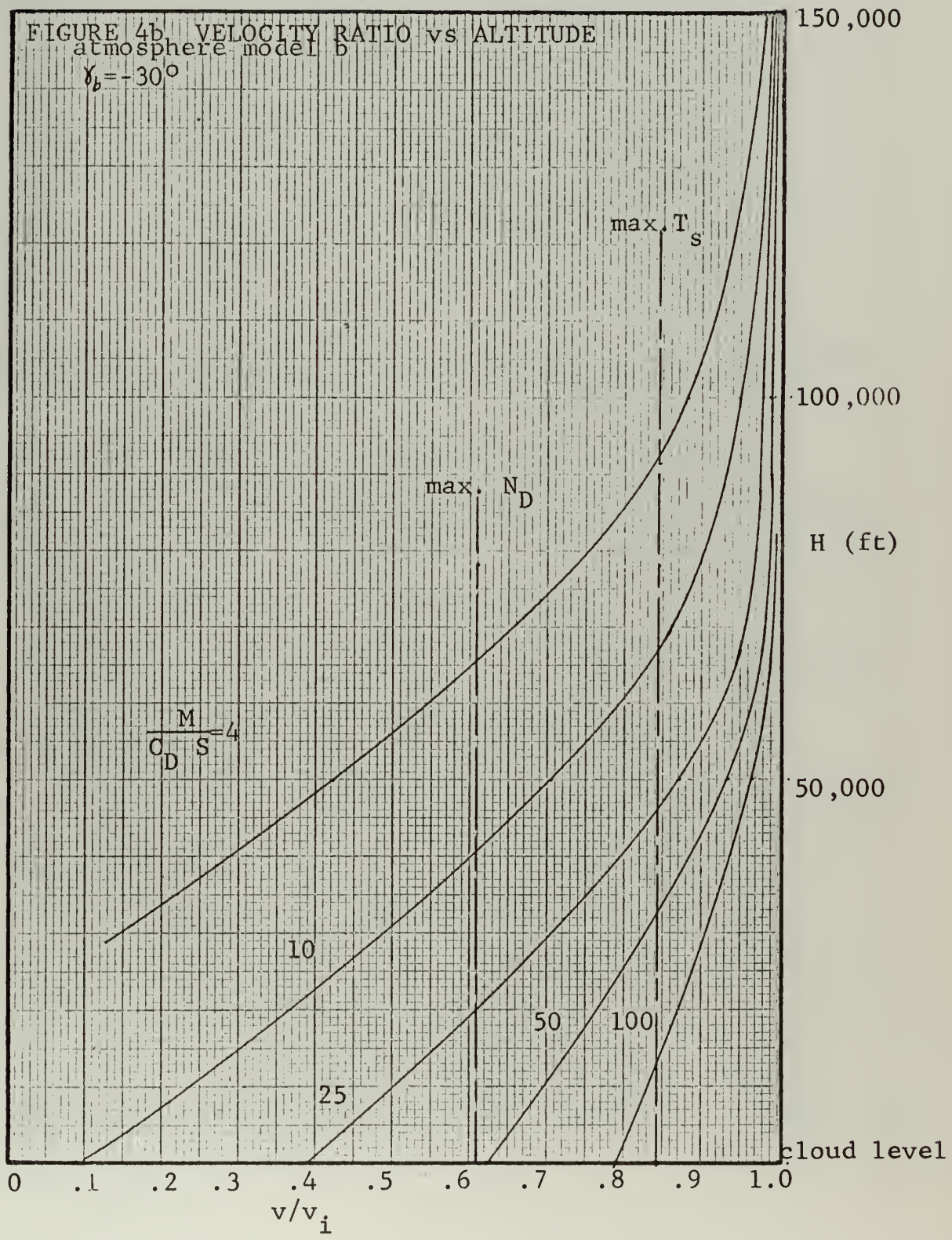
FIGURE 4b VELOCITY RATIO vs ALTITUDE
atmosphere model b
$\gamma_b = -30^o$
max. T_s
max. N_D
$\frac{M}{C_D S} = 4$
10
25
50
100
150,000
100,000
50,000
H (ft)
cloud level
0
.1
.2
.3
.4
.5
.6
.7
.8
.9
1.0
v/v_i

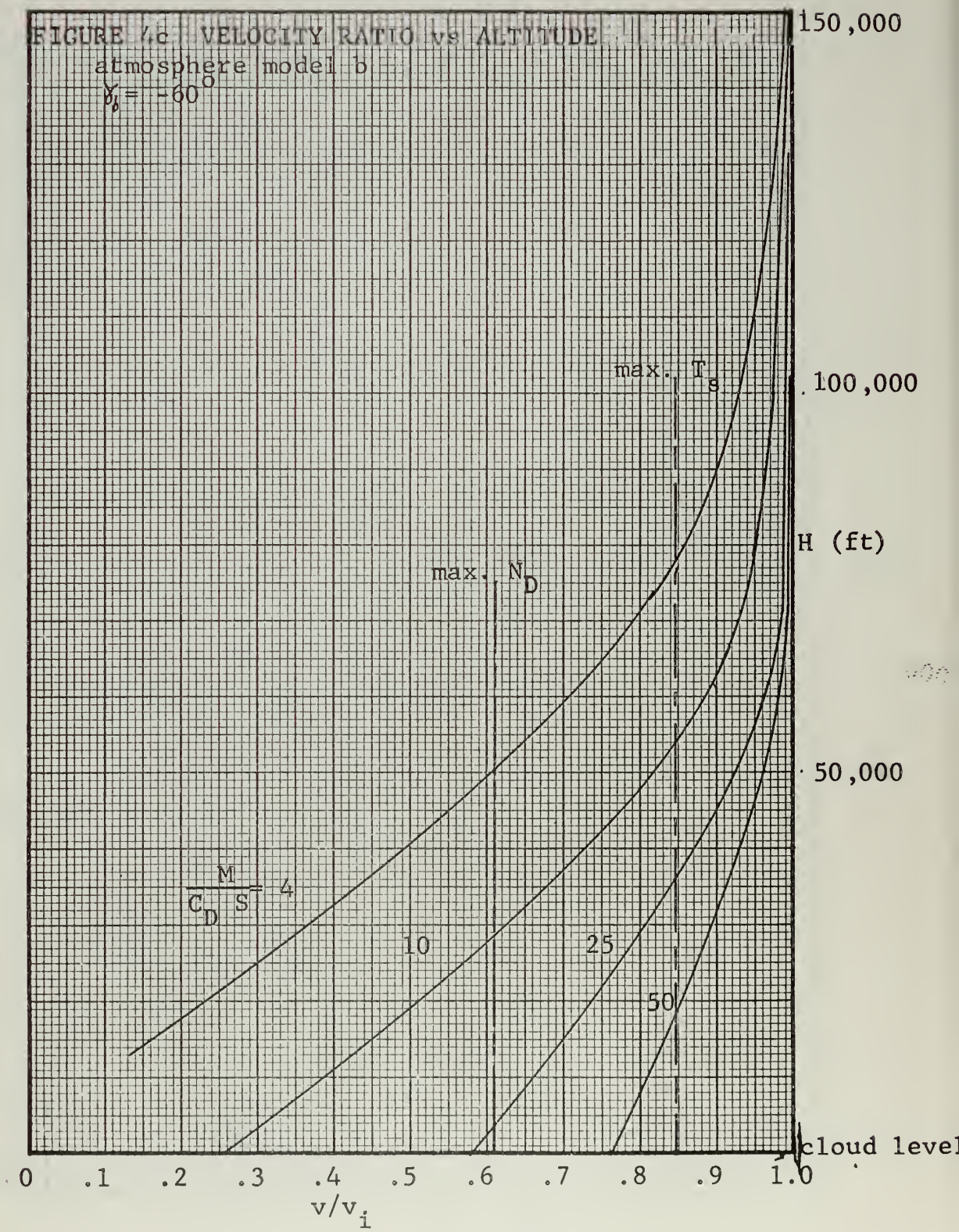
FIGURE 4c VELOCITY RATIO vs ALTITUDE
atmosphere model b
$\gamma_0 = -60^0$
150,000
100,000
50,000
H (ft)
max. T_s
max. N_D
$\frac{M}{C_D S} = 4$
10
25
50
cloud level
0
.1
.2
.3
.4
.5
.6
.7
.8
.9
1.0
v/v_i

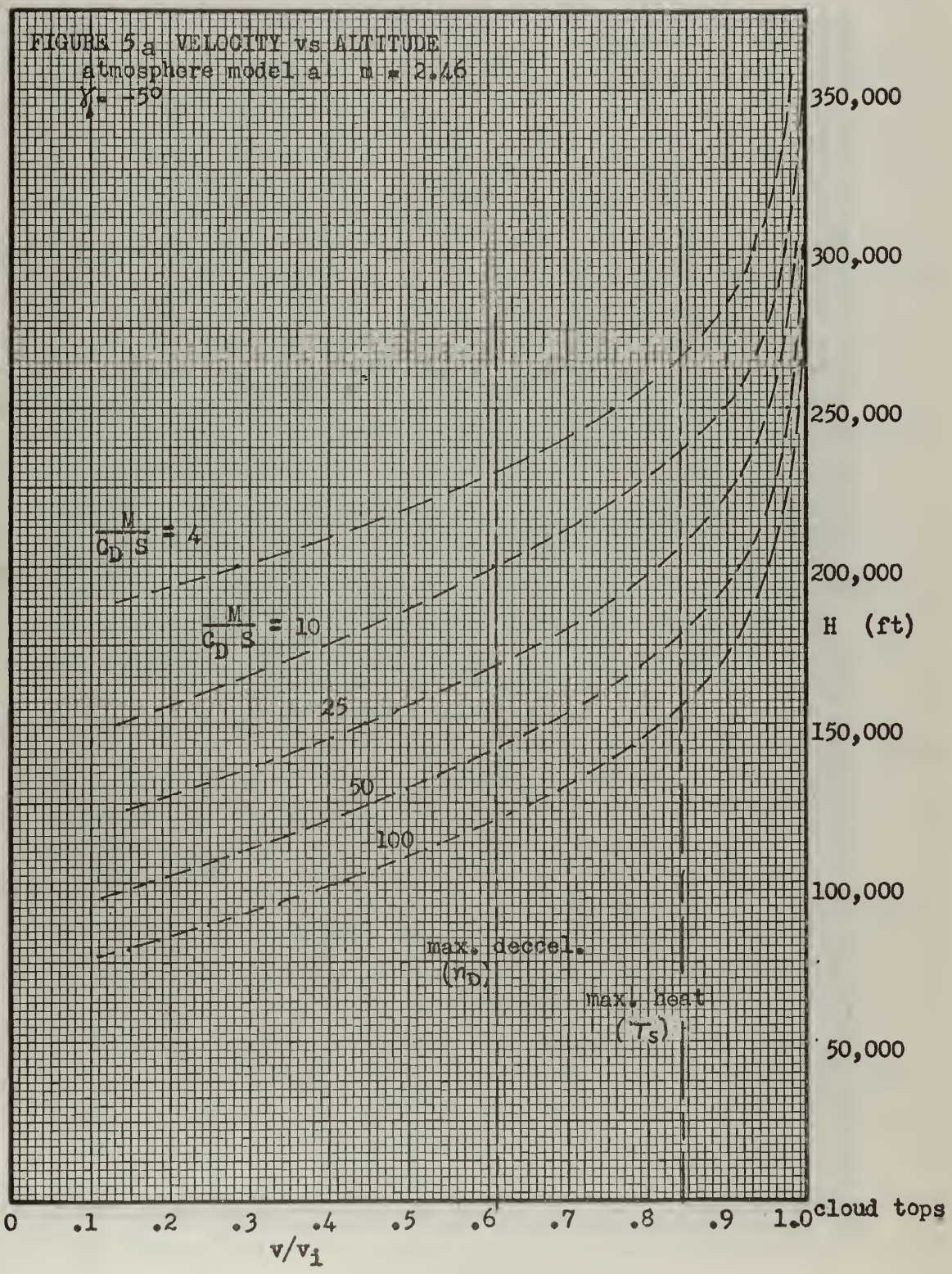
FIGURE 5a VELOCITY vs ALTITUDE
atmosphere model a m = 2.46
γ_i = -5°
$\frac{M}{C_D S}$ = 4
$\frac{M}{C_D S}$ = 10
25
50
100
max. deccel. (r_D)
max. heat (T_s)
350,000
300,000
250,000
200,000
H (ft)
150,000
100,000
50,000
cloud tops
0
.1
.2
.3
.4
.5
.6
.7
.8
.9
1.0
v/v_i

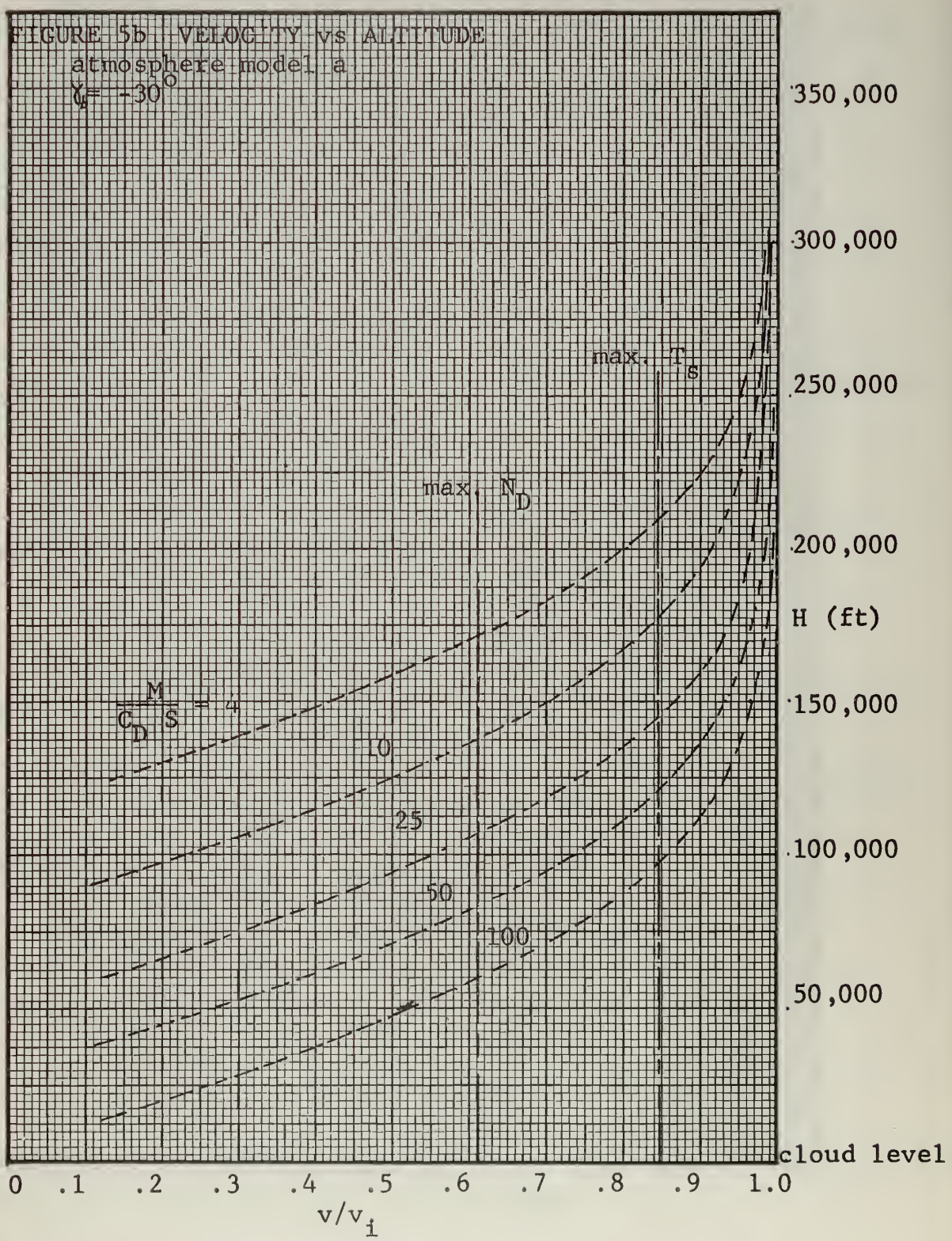
FIGURE 5b VELOCITY vs ALTITUDE
atmosphere model a
$\gamma_i = -30^\circ$
350,000
300,000
250,000
200,000
H (ft)
150,000
100,000
50,000
cloud level
max. T_s
max. N_D
$\frac{M}{C_D S} = 4$
10
25
50
100
0 .1 .2 .3 .4 .5 .6 .7 .8 .9 1.0
v/v_i

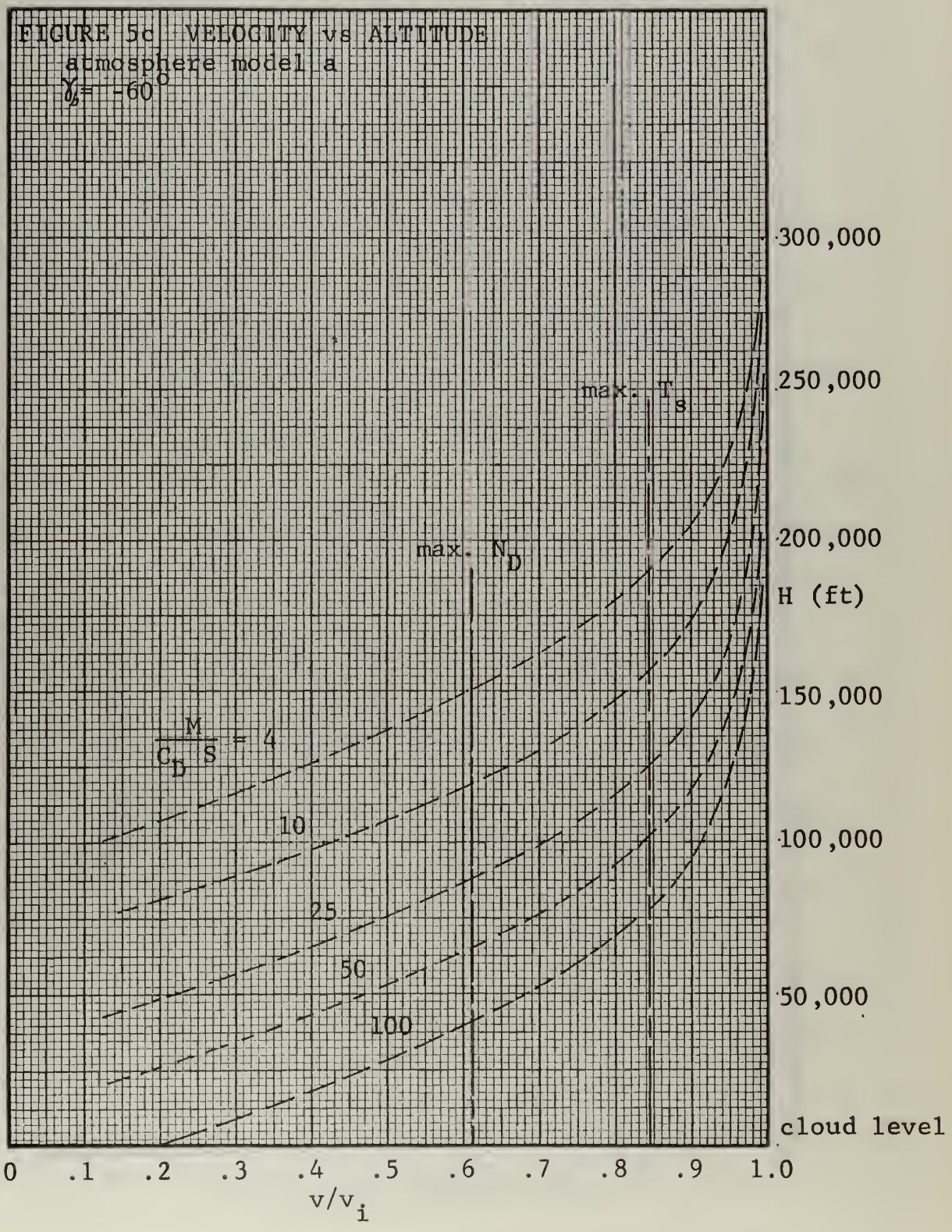
FIGURE 5c VELOCITY vs ALTITUDE
atmosphere model a
$\gamma_s = -60^0$
max. T_s
max. N_D
$\frac{M}{C_D S} = 4$
10
25
50
100
300,000
250,000
200,000
H (ft)
150,000
100,000
50,000
cloud level
0
.1
.2
.3
.4
.5
.6
.7
.8
.9
1.0
v/v_i

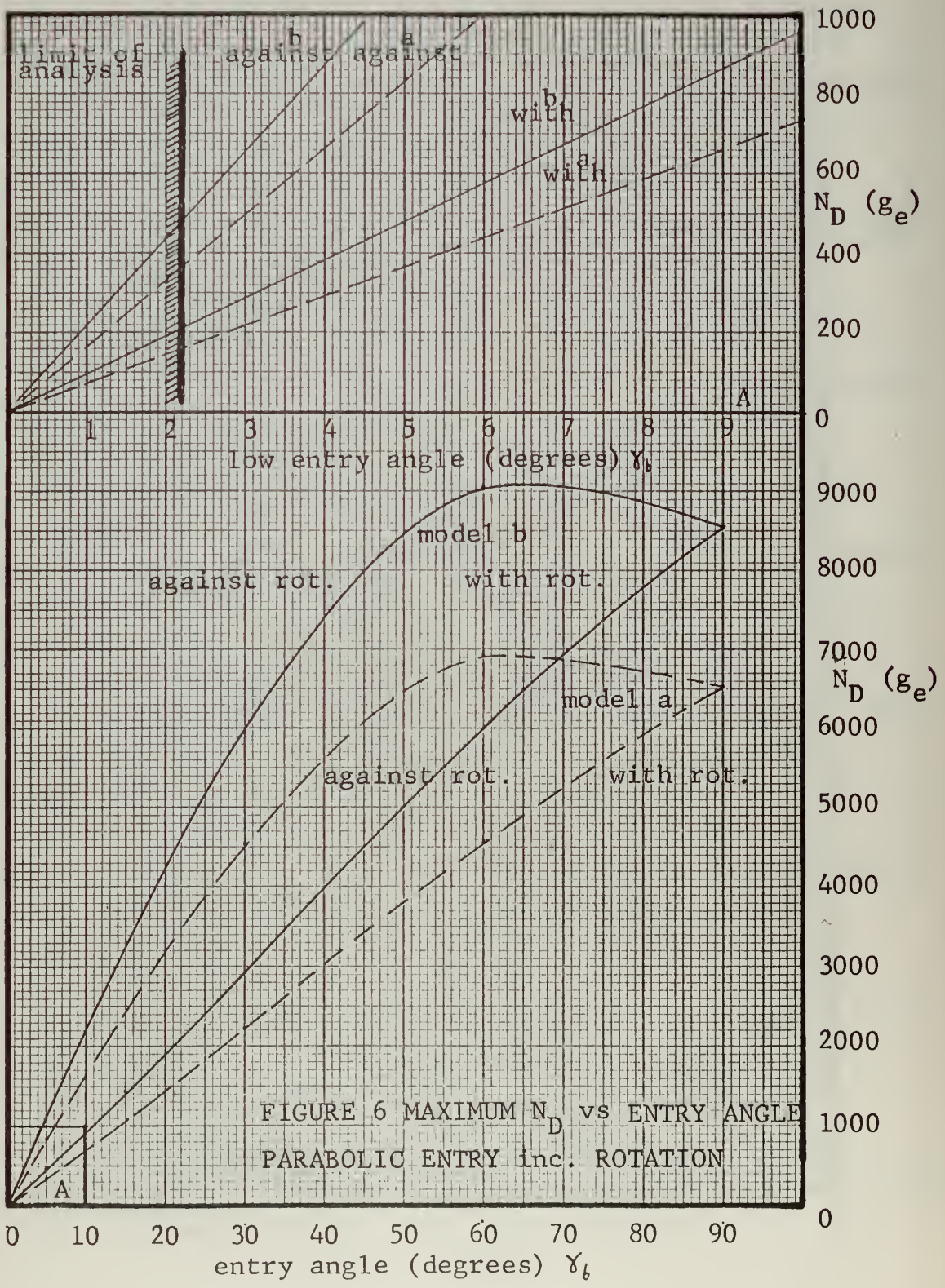

FIGURE 6 MAXIMUM N_D vs ENTRY ANGLE
PARABOLIC ENTRY inc. ROTATION

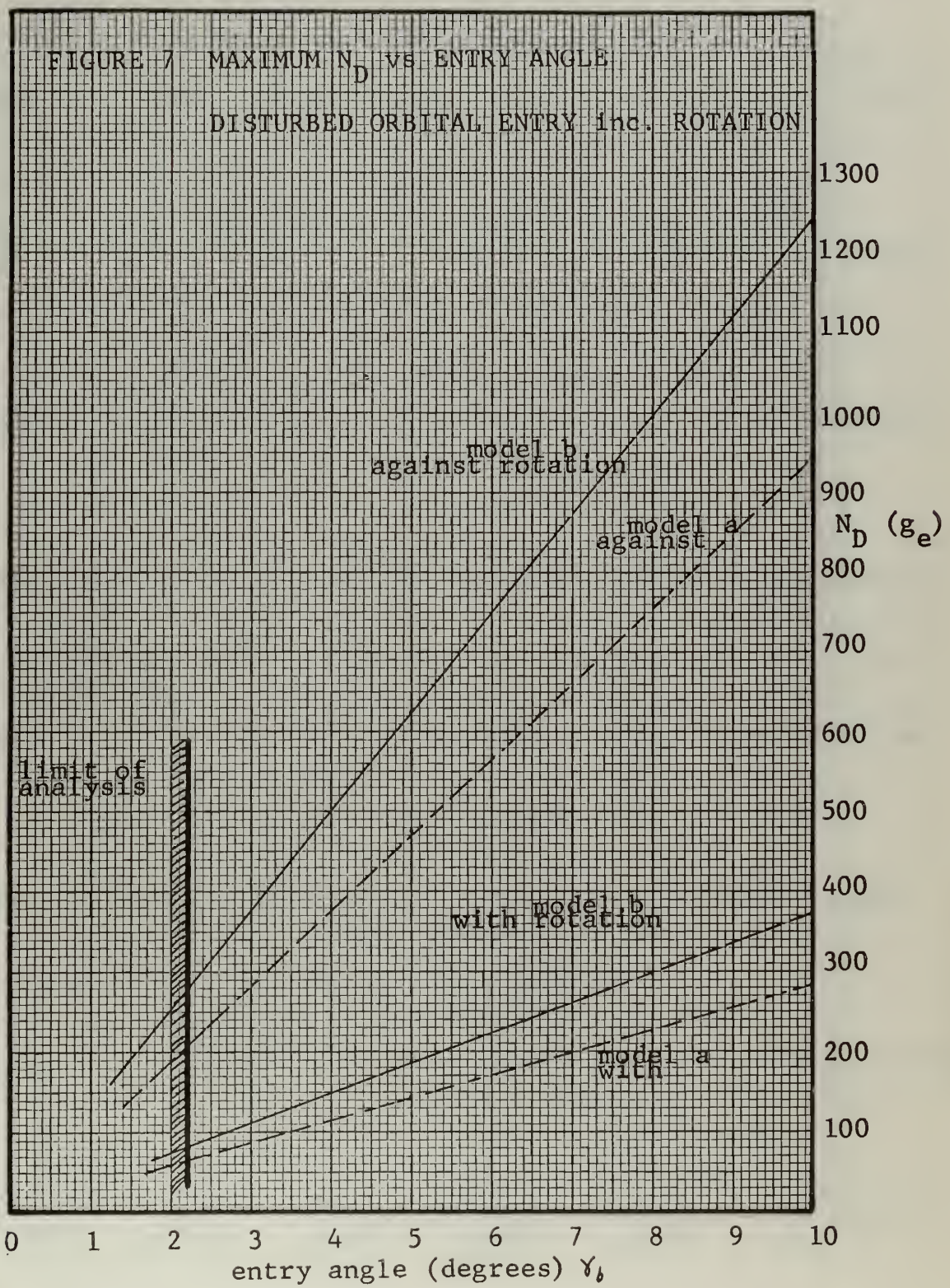
FIGURE 7 MAXIMUM N_D vs ENTRY ANGLE
DISTURBED ORBITAL ENTRY inc. ROTATION
1300
1200
1100
1000
900
800
700
600
500
400
300
200
100
N_D (g_e)
model b against rotation
model a against
limit of analysis
model b with rotation
model a with
0 1 2 3 4 5 6 7 8 9 10
entry angle (degrees) γ_i

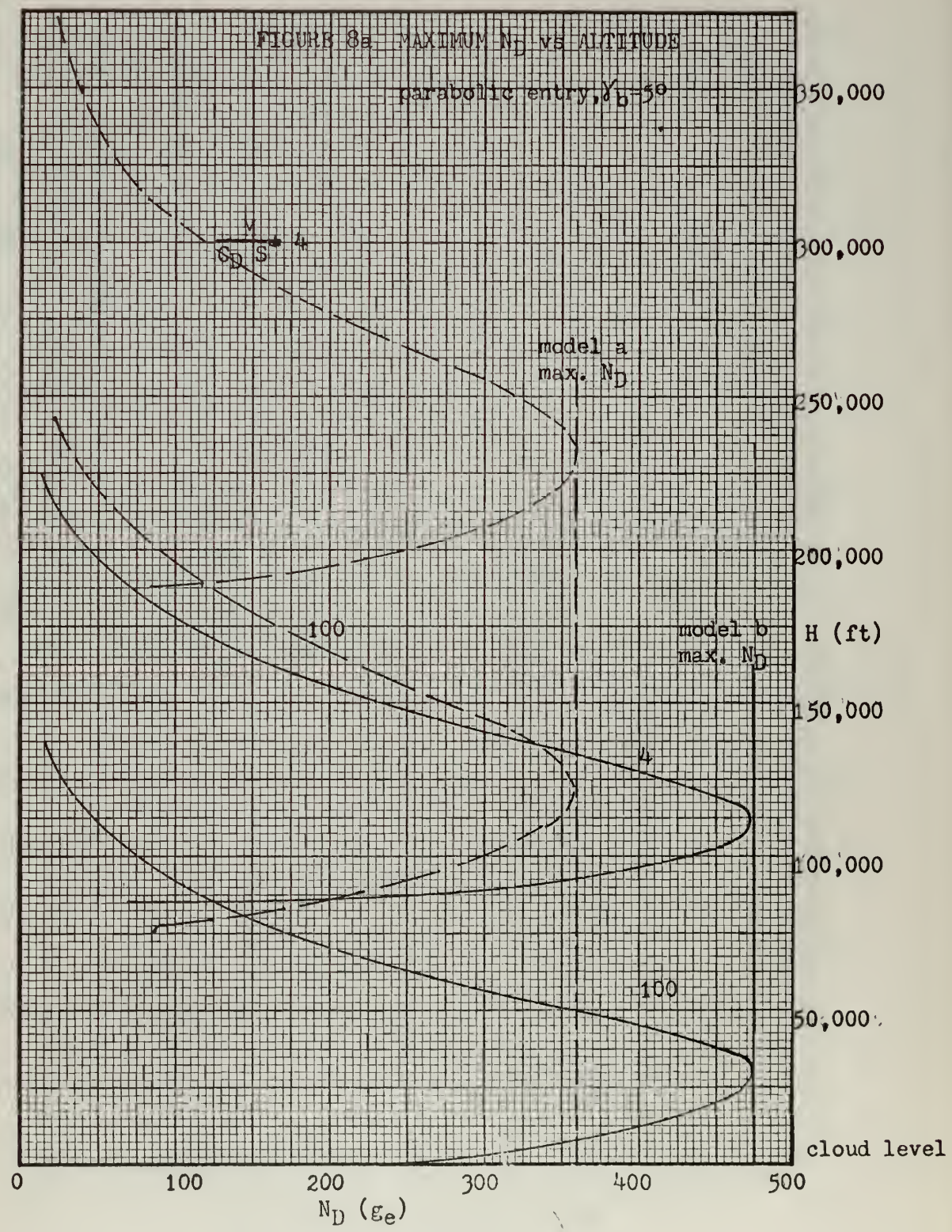
FIGURE 8a MAXIMUM N_D vs ALTITUDE
parabolic entry, $\gamma_b = 5^o$
$\frac{M}{C_D S} = 4$
model a
max. N_D
model b
max. N_D
100
4
100
350,000
300,000
250,000
200,000
150,000
100,000
50,000
H (ft)
cloud level
0
100
200
300
400
500
N_D (g_e)

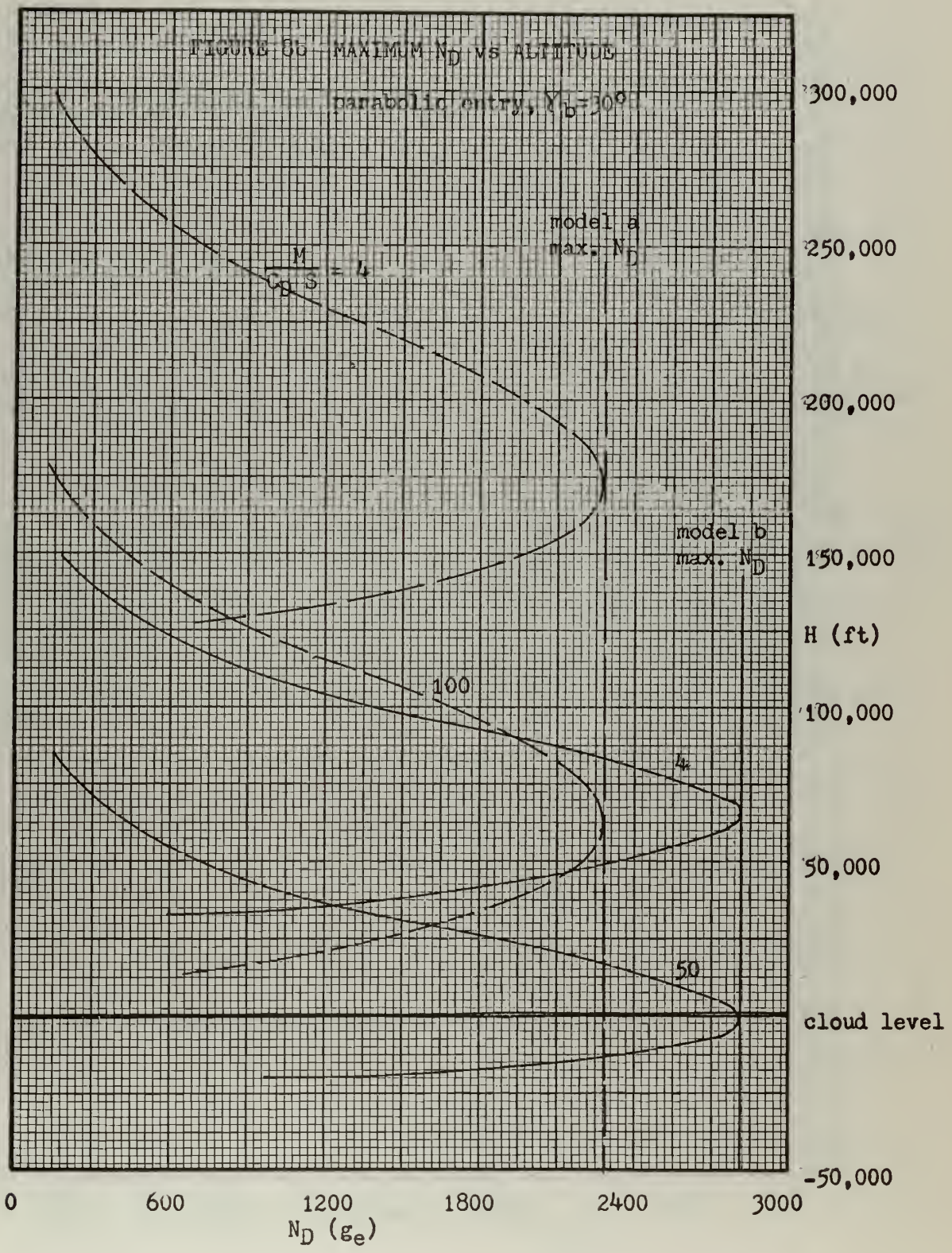
FIGURE 66 - MAXIMUM N_D VS ALTITUDE
parabolic entry, $\gamma_b = 30°$
$\frac{M}{C_D S} = 4$
model a
max. N_D
model b
max. N_D
100
4
50
300,000
250,000
200,000
150,000
H (ft)
100,000
50,000
cloud level
-50,000
0
600
1200
1800
2400
3000
N_D (g_e)

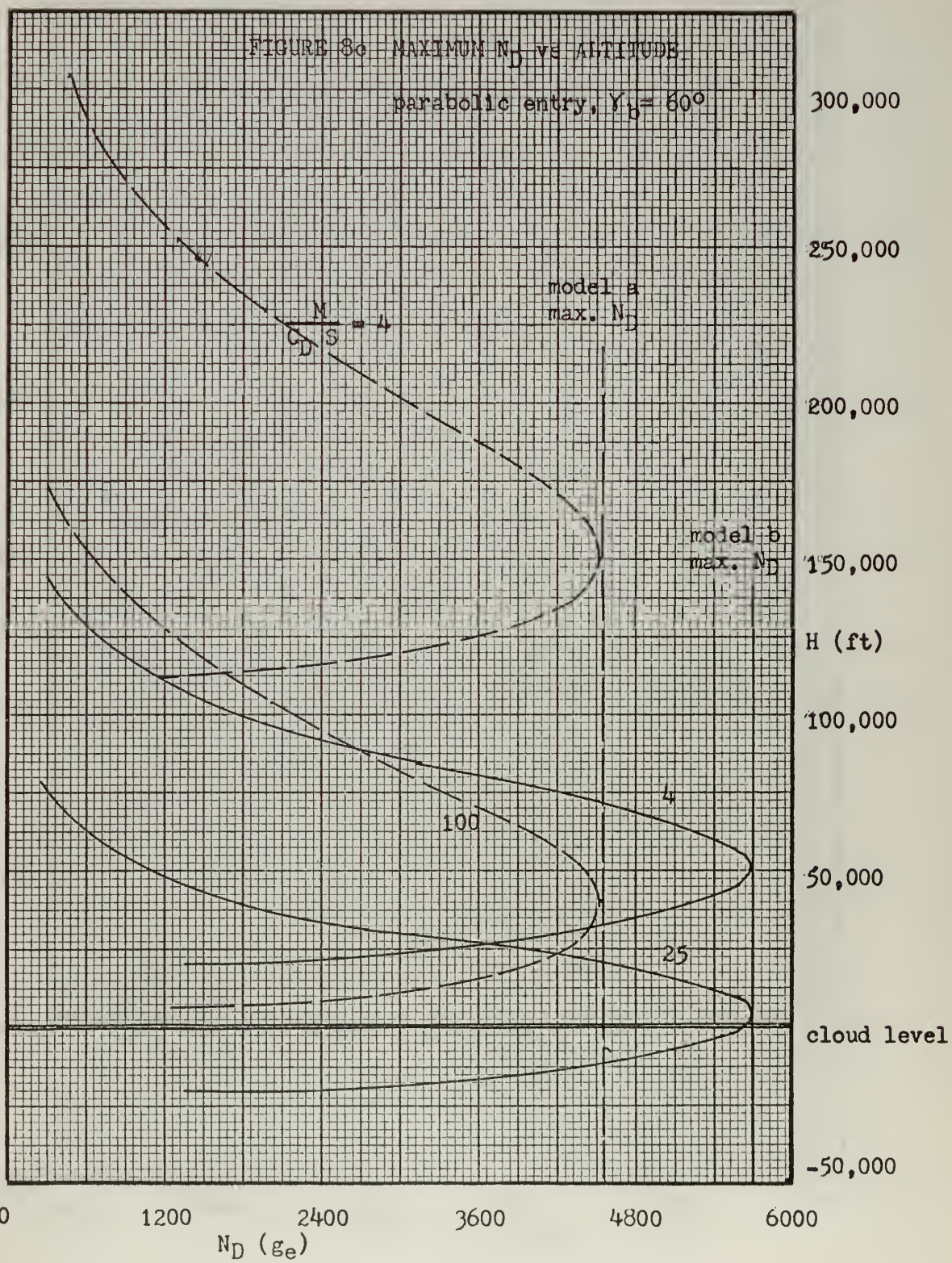
FIGURE 8c MAXIMUM N_D vs ALTITUDE
parabolic entry, $\gamma_b = 60°$
$\frac{M}{C_D S} = 4$
model a max. N_D
model b max. N_D
100
4
25
300,000
250,000
200,000
150,000
H (ft)
100,000
50,000
cloud level
-50,000
0
1200
2400
3600
4800
6000
N_D (g_e)

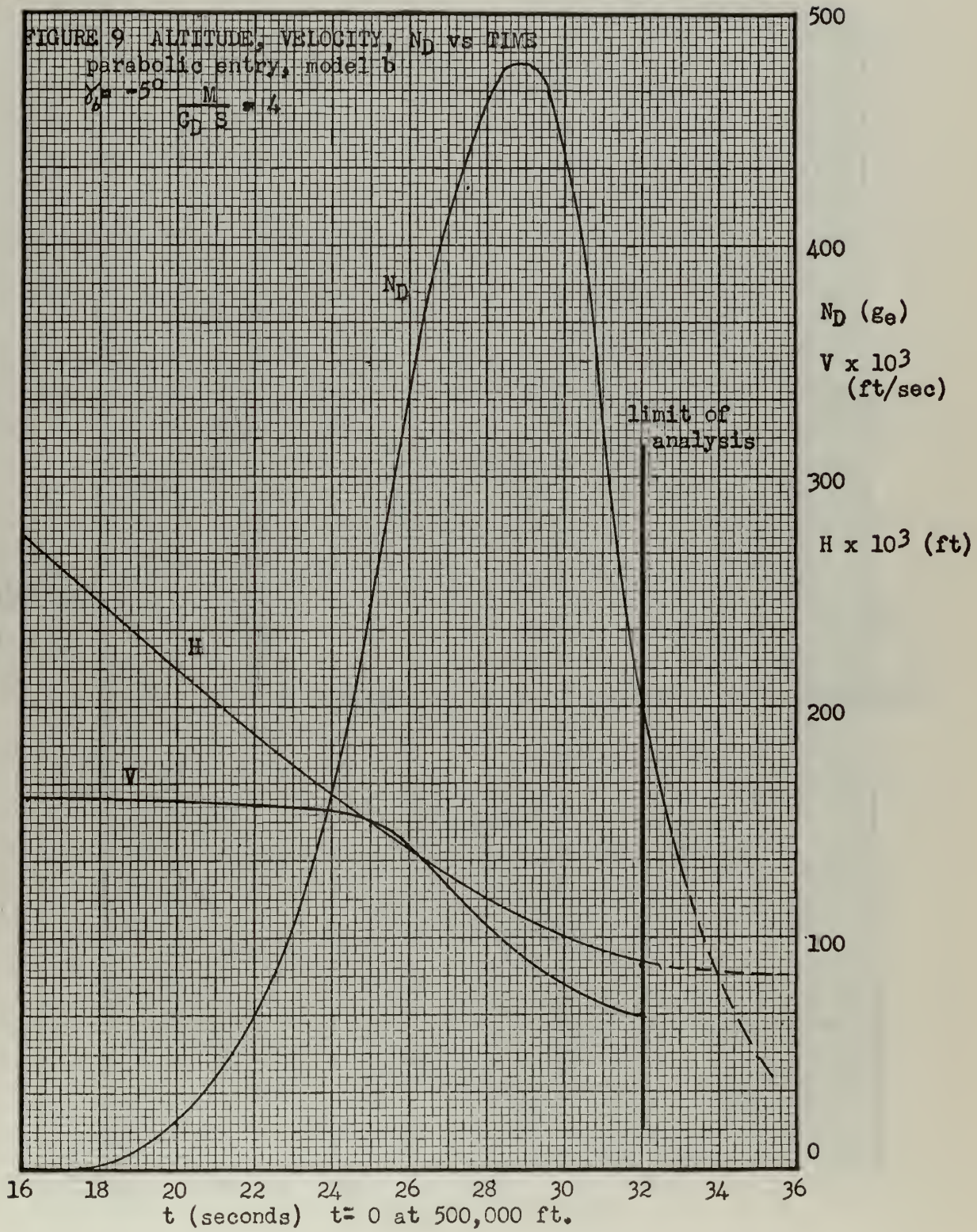
FIGURE 9 ALTITUDE, VELOCITY, N_D vs TIME
parabolic entry, model b
$\gamma_i = -5^o$
$\frac{M}{C_D S} = 4$
N_D
H
V
limit of analysis
500
400
300
200
100
0
N_D (g_e)
V x 10^3 (ft/sec)
H x 10^3 (ft)
16
18
20
22
24
26
28
30
32
34
36
t (seconds) t= 0 at 500,000 ft.

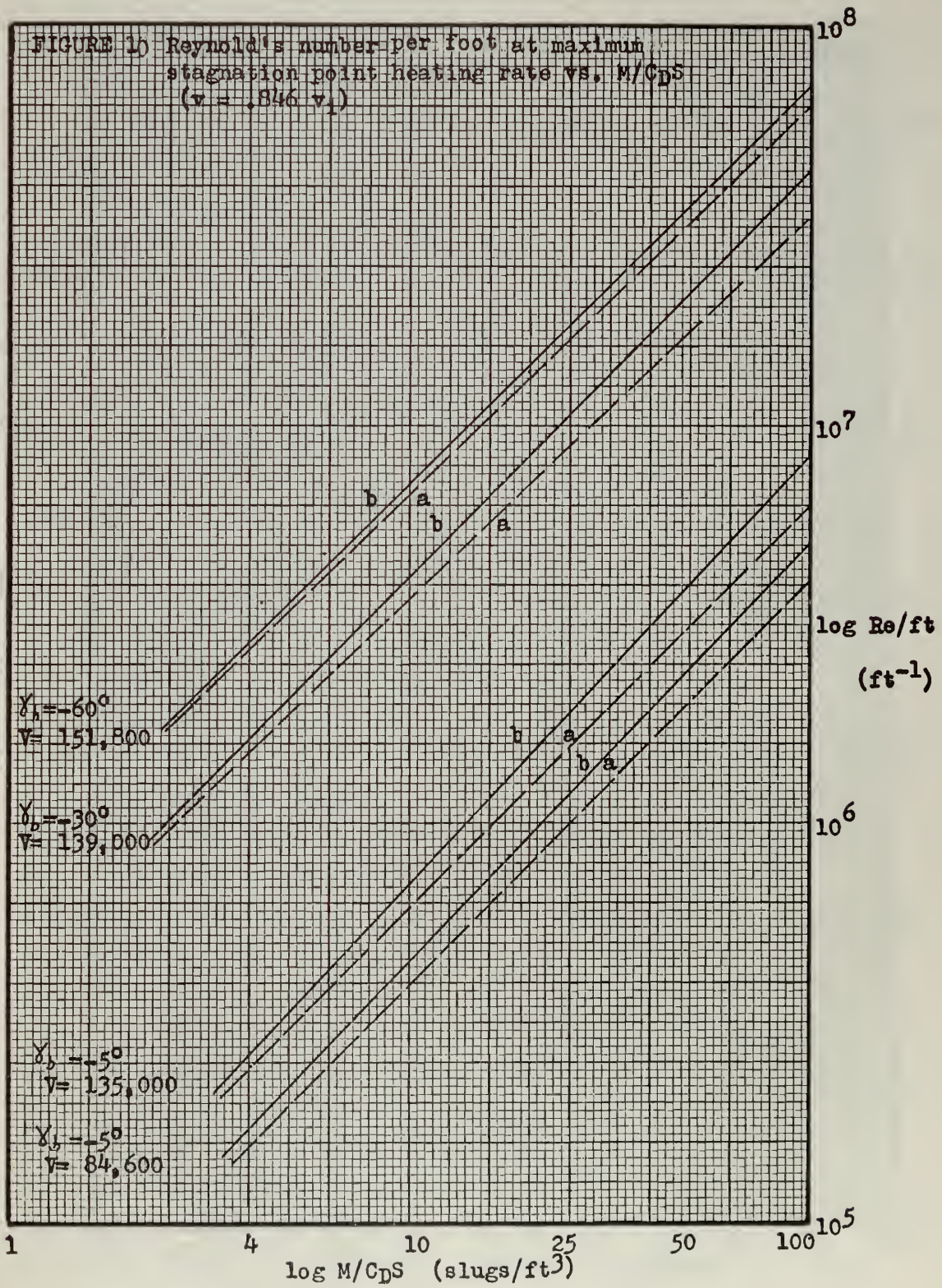
FIGURE 20 Reynold's number per foot at maximum stagnation point heating rate vs. M/C_DS (v = .846 v_1)
10^8
10^7
10^6
10^5
log Re/ft (ft^-1)
γ_b=-60°
V= 151,800
γ_b=-30°
V= 139,000
γ_b =-5°
V= 135,000
γ_b =-5°
V= 84,600
b a
b a
b a
b a
1
4
10
25
50
100
log M/C_DS (slugs/ft^3)

FIGURE 11 MAXIMUM STAGNATION AREA HEATING RATE vs M/C_DS

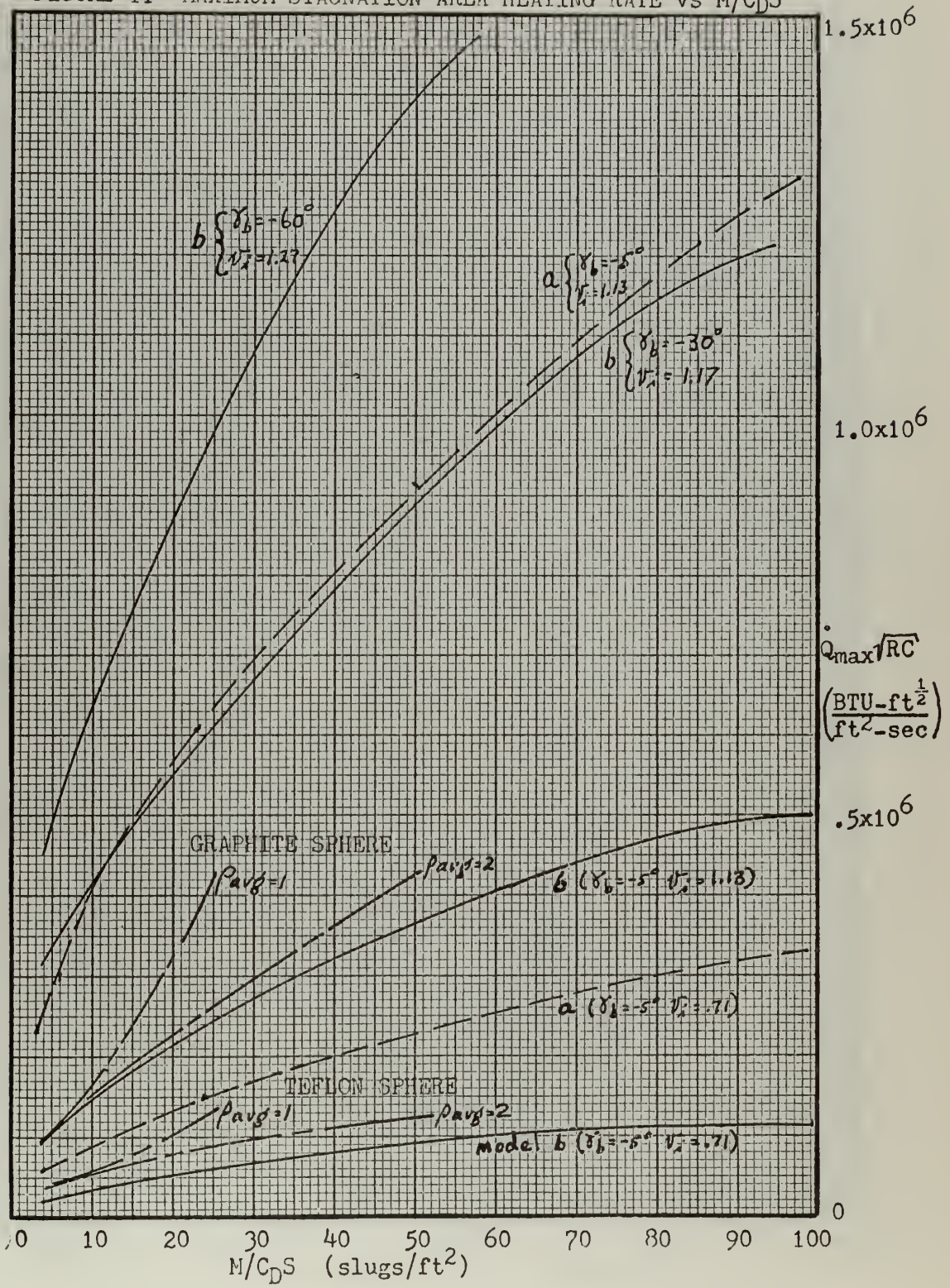

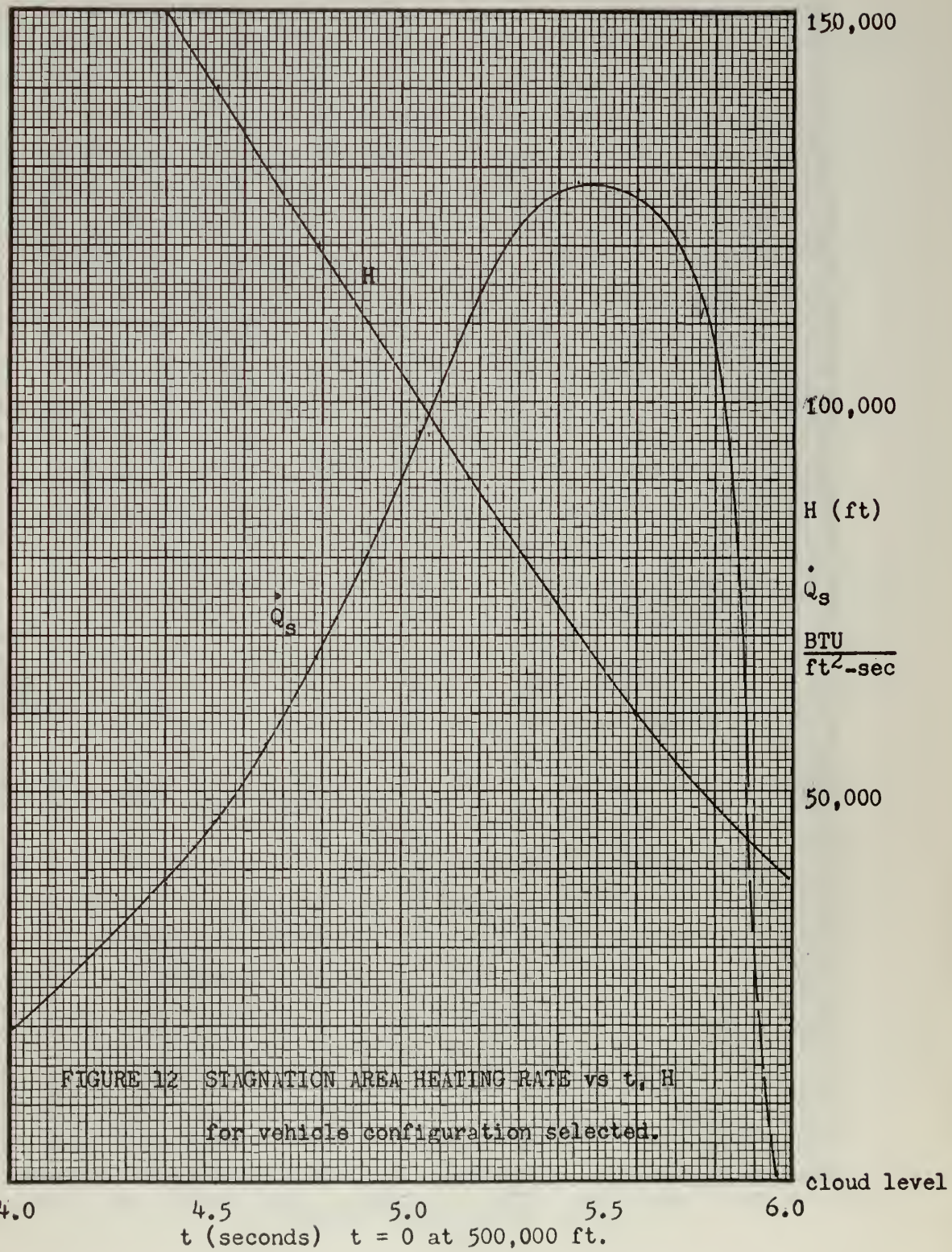

FIGURE 12 STAGNATION AREA HEATING RATE vs t, H

for vehicle configuration selected.

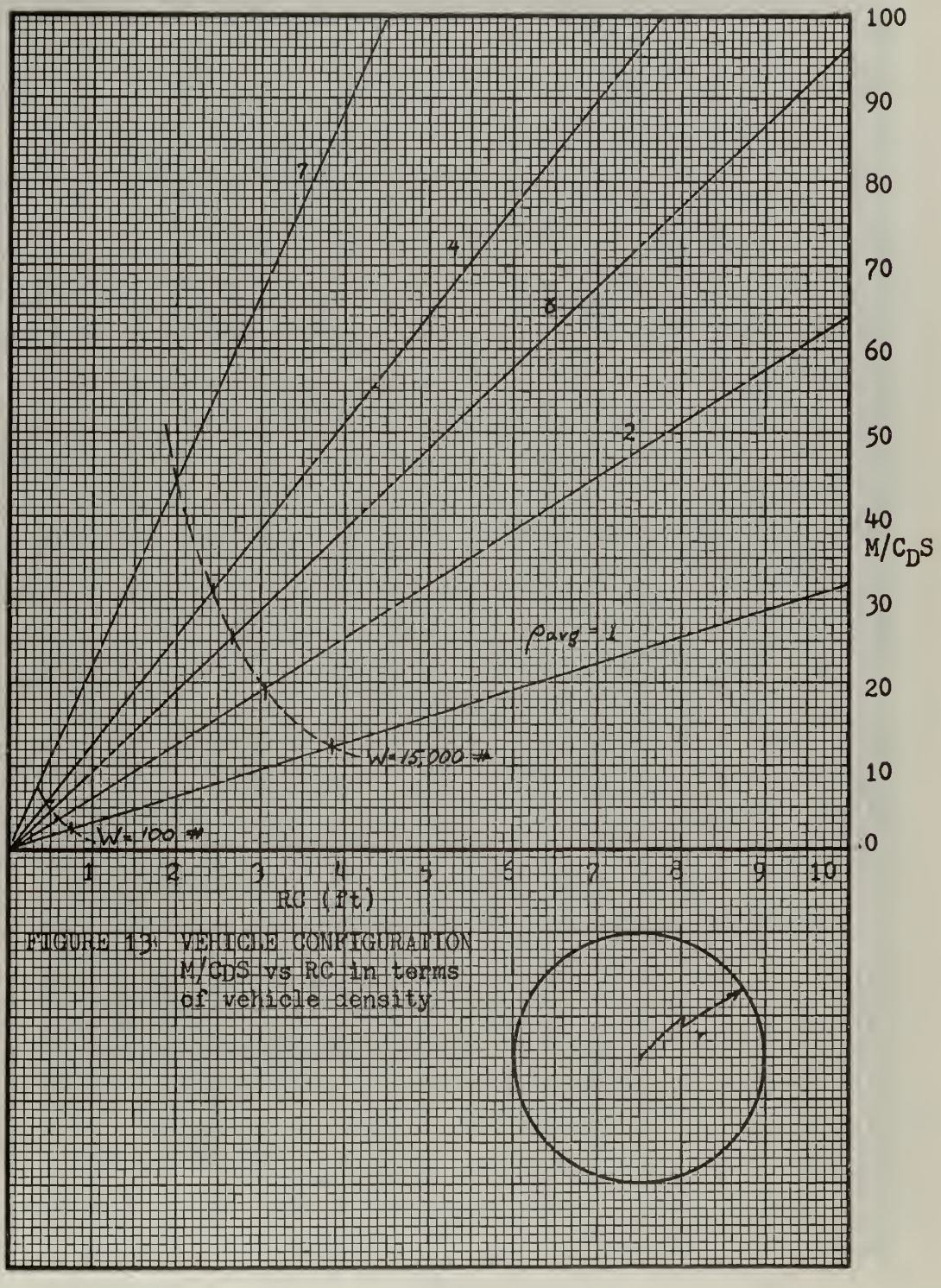

FIGURE 13 VEHICLE CONFIGURATION M/CDS vs RC in terms of vehicle density

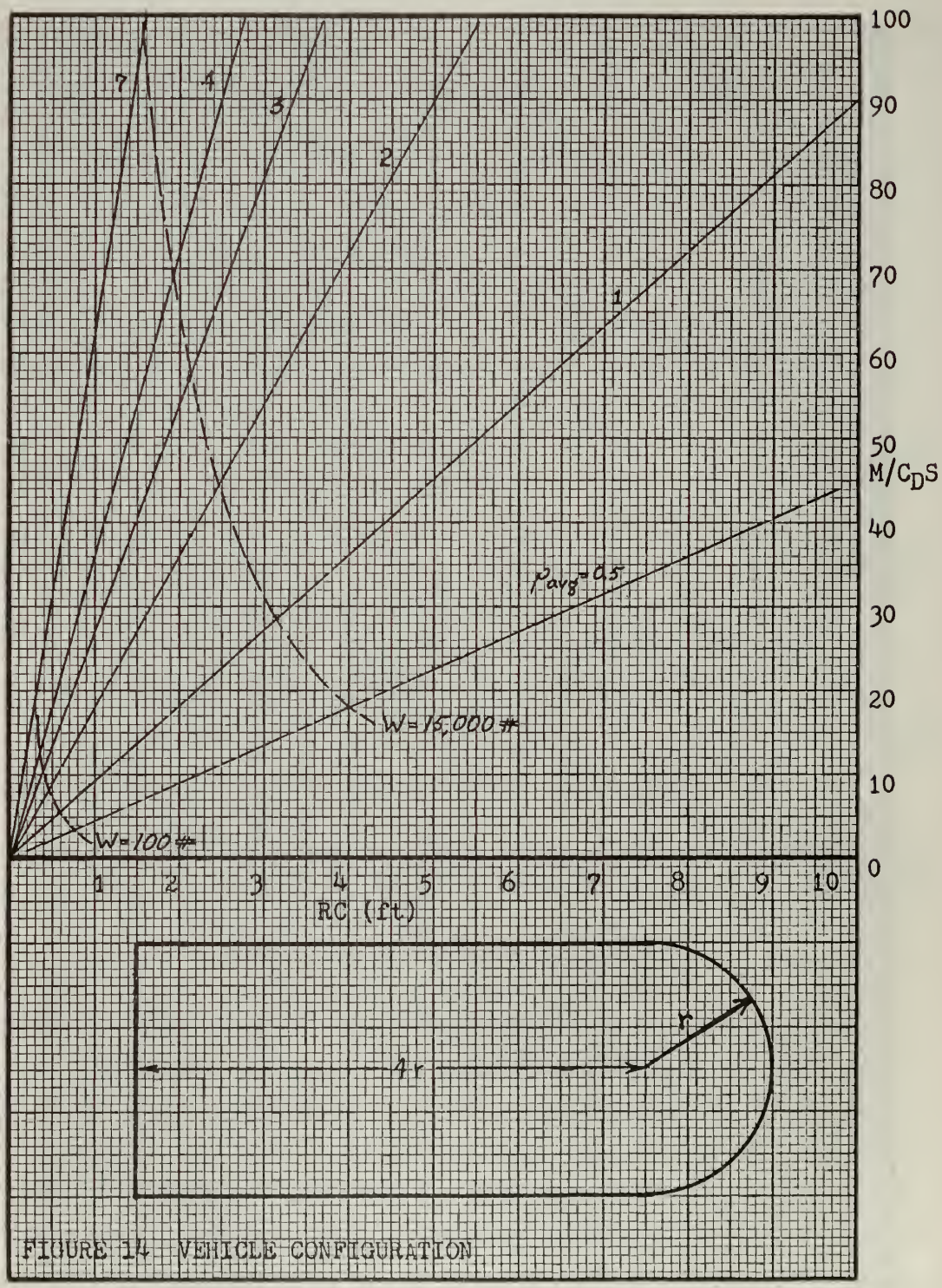

FIGURE 14 VEHICLE CONFIGURATION

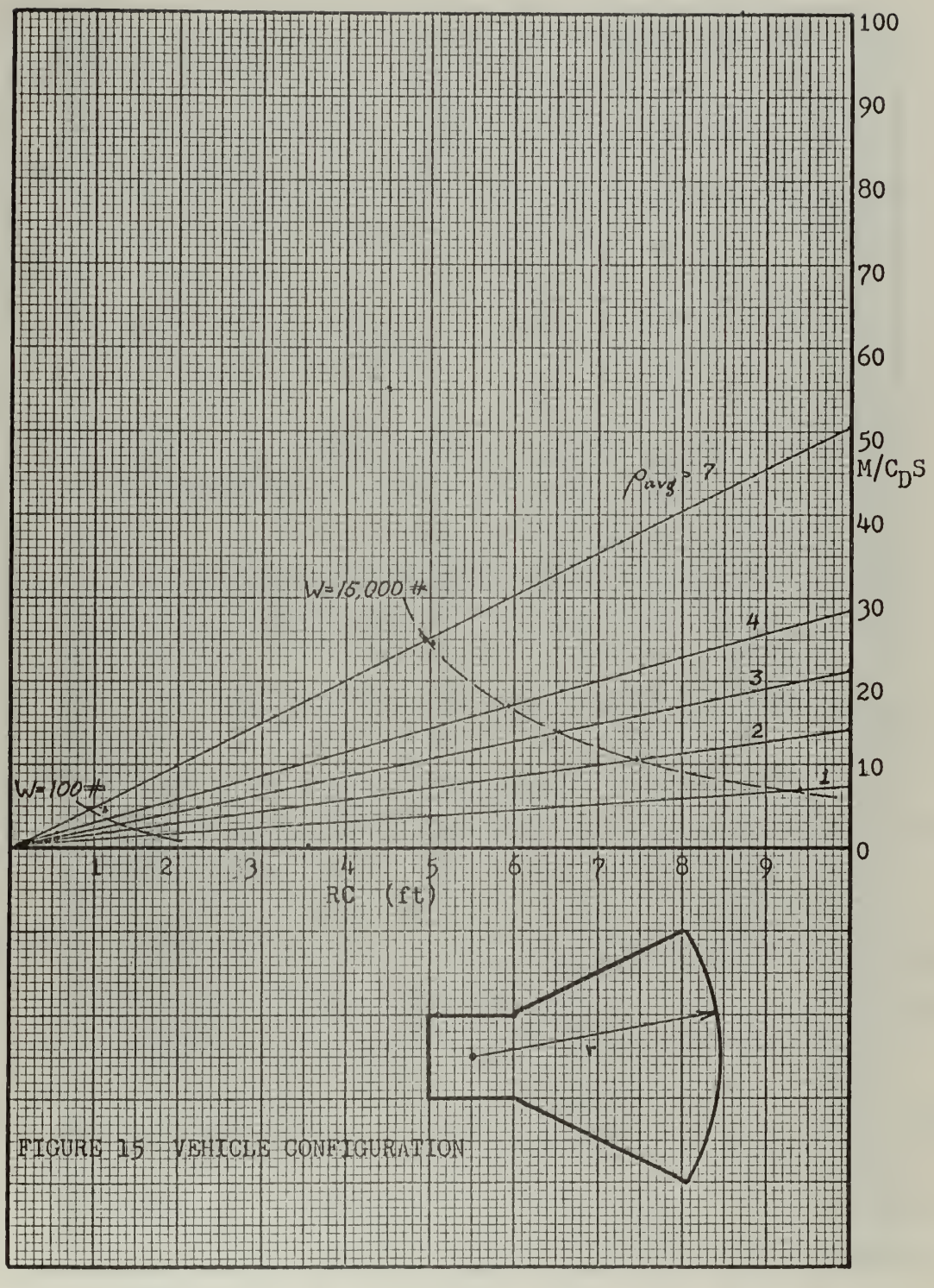

FIGURE 15 VEHICLE CONFIGURATION

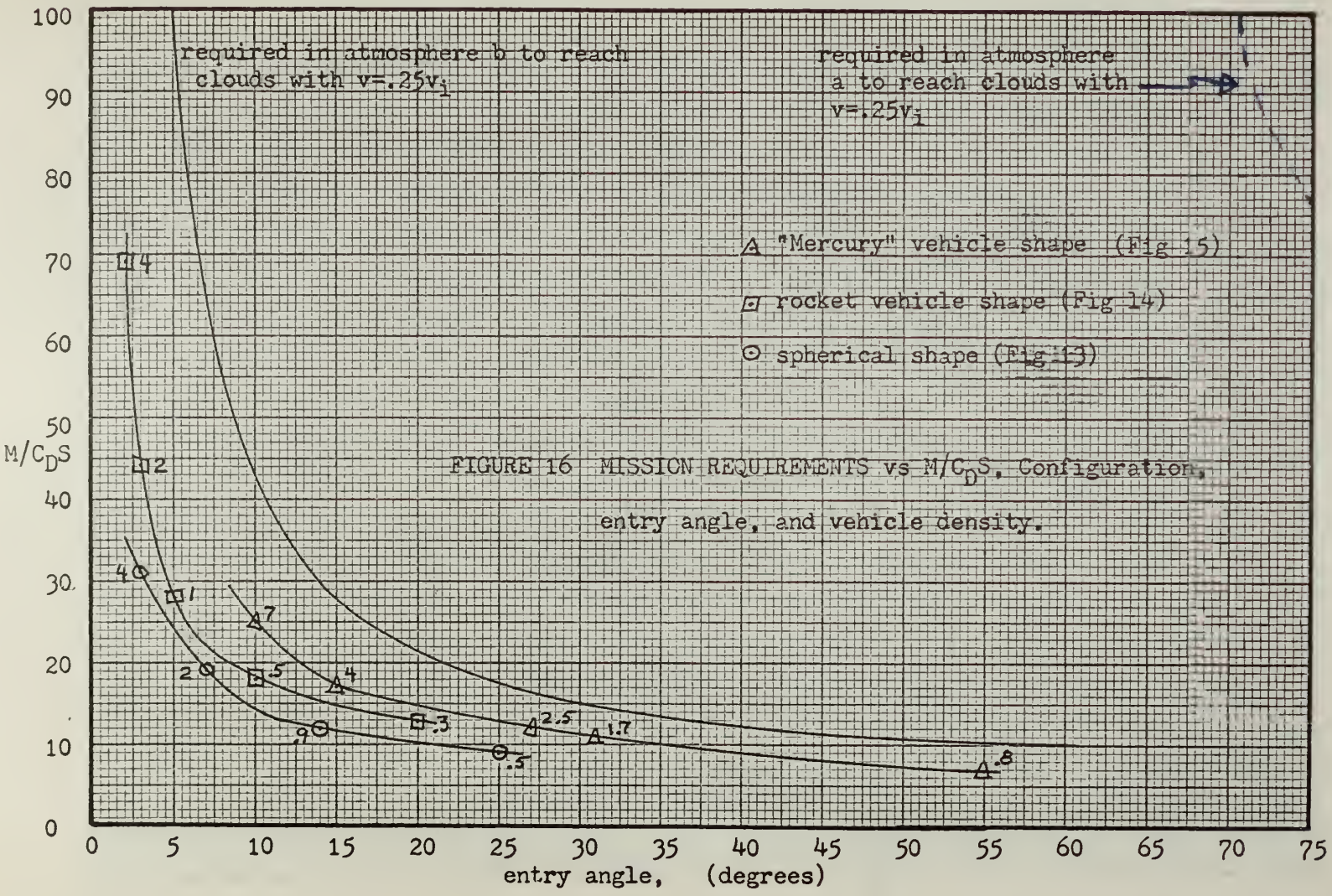

FIGURE 16 MISSION REQUIREMENTS vs M/C_DS, Configuration, entry angle, and vehicle density.

REFERENCES

1. Kuiper, G.P., "The Atmospheres of the Earth and Planets", University of Chicago Press, 1952.

2. "Handbuch der Physik", S. Flugge, ed., vol 52, Springer-Verlag, Berlin, 1959.

3. Jeans, J.H., "The Dynamical Theory of Gases", Cambridge University Press, Cambridge, 1925.

4. "Encyclopaedia Britannica", William Benton, ed., vol 13, pp 190, Chicago, 1959.

5. Peek, B.M., "The Planet Jupiter", Faber and Faber, London, 1959.

6. Duncan, R.C., "Guidance Parameters and Constraints for Controlled Atmospheric Entry," MIT Instrumentation Lab Report T-235, 1960.

7. Chapman, D.R., "An Approximate Analytical Method for Studying Entry into Planetary Atmospheres", NASA T.R. R-11, Washington, 1959.

8. "Ablation Cooling", bulletin 160, CTL Corp., Cincinnati, 1960.

9. Gazley, C., and Masson, D.J., "Surface Protection and Cooling Systems for High-Speed Flight", IAS Preprint #638, New York, 1956.

BIBLIOGRAPHY

A. Atmospheres and Physical Constants

1. Romer, E.M., "Planetary Atmospheres and some Associated Flight Problems", unpublished notes, MIT, 1959.

2. "Space Technology", H. Seifert, ed., John Wiley and Sons, New York, 1959.

3. Firsoff, V.A., "Dissipation of Planetary Atmospheres", Science, vol 130, No. 3385, pp 1337, 13 Nov 1959.

4. Urey, H.C., "The Planets, Their Origin and Development", Yale University Press, New Haven, 1952.

5. Struve, O., "The Atmospheres of Jupiter and Saturn," Sky and Telescope, vol XIII, No. 10, pp 336, Aug 1954.

B. Heating and Deceleration

1. Allen, H.J., and Eggers, A.J., Jr., "A Study of the Motion and Aerodynamic Heating of Missiles Entering the Earth's Atmosphere at High Supersonic Speeds", NACA TR 1381, 1958.

2. Eggers, A.J. Jr., and Allen, H.J., "A Comparative Analysis of the Performance of Long Range Hypervelocity Vehicles", NACA TR 1382, 1958.

3. Detra, R.W., Kemp, N.H., and Riddell, F.R., "Heat Transfer to Satellite Vehicles Re-entering the Atmosphere", Jet Propulsion, Vol 27, No. 2 (Feb 57), and addendum, No 12 (Dec 57).

4. Eggleston, J.M., and Cheatham, D.C., "Piloted Entries into the Earth's Atmosphere", IAS Paper No. 59-98, New York, 1959.

5. Detra, R.W., and Riddell, F.R., "Controlled Recovery of Non-Lifting Satellites", ARS Paper 784-59, 1959.

6. Gazley, C.Jr., "Deceleration and Heating of a Body Entering a Planetary Atmosphere from Space", Rand Report P-955, 1957.

7. Kepler, D.I., "Concepts Influencing the Selection of a Configuration for Atmospheric Re-entry", ARS Paper 786-59, 1959.

8. Sandorff, P.E., Unpublished notes for Course 16·761, "Orbital Vehicles," MIT, 1959.

9. Rubensin, M.W., "The Influence of Aerodynamic Heating on the Structural Design of Aircraft", VIDYA Associates, Palo Alto, 1958.

10. Lees, L., "Laminar Heat Transfer Over Blunt-Nosed Bodies at Hypersonic Flight Speeds", Jet Propulsion, Vol 26, No.4, 1956.

11. Romig, Mary F., "Stagnation Point Heat Transfer for Hypersonic Flow," Jet Propulsion, vol 26, No. 12, 1956.